Neutron Yields from Individual Fission Fragments*

JAMES TERRELL
Los Alamos Scientific Laboratory, University of California, Los Alamos, New Mexico
(Received March 12, 1962)

Two new methods are used to obtain data on neutron yield ν_f as a function of the mass number M of the emitting fission fragment; the results suggest changes in fission theory. The methods involve the combination of data on fission mass yields obtained by radiochemical means with time-of-flight mass data. The more detailed method yields essentially the complete function $\nu_f(M)$. Both methods are applied to neutron fission of U^{233}, U^{235}, and Pu^{239}, and to spontaneous fission of Cf^{252}. The neutron yields obtained, which show strong variation with mass, are compared with other available data; no previous results exist for Pu^{239}. The four sets of data on $\nu_f(M)$ are so similar that it is suggested that the neutron yield is primarily a function of fragment mass and not of mass ratio. In each case minimum neutron yield is found for $N\cong 50$ and $Z=\cong 50$ (masses 82 and 128). It is suggested that these magic and near-magic fragments have low excitations, and consequently emit almost no neutrons, because of greater rigidity against distortion from near-spherical shapes. The same idea leads to a prediction of high fission barrier and low fission yield at these masses, which compares well with data for single-peaked, triple-peaked, and ordinary double-peaked-mass-yield fission. In the appendices a number of necessary relations are developed, concerning neutron emission energies. The width of the neutron emission spectrum is deduced from laboratory spectra; new relations between emission spectra and angular correlation of neutrons and fragments are developed and applied; and it is shown that the extra width of fragment mass yields obtained from fragment energies (semiconductor or ionization-chamber data) is due to the correlation of ν_f and M.

I. INTRODUCTION

SINCE 1954 there has been experimental evidence, of increasing weight, that the neutron yield from fission fragments is not simply equally divided between light and heavy fragments, but is a more complicated function of fragment mass. For low-mass-ratio fission most of the neutrons come from the light fragment, while the reverse is true for high mass ratios. The available data are summarized and, where possible, corrected in this paper. However, such direct measurements of neutron yield are difficult to do with sufficient accuracy and suffer from uncertainty in the corrections for angular correlations of the neutrons. This correction, and others, are discussed in the appendices, which summarize information related to neutron energies.

It is the main purpose of this paper to indicate two new methods of determining the neutron yield by using mass-yield data alone, and to give the results obtained so far. One method uses moments and covariances; the other method uses cumulative distributions. In the case of neutron fission of Pu^{239}, the neutron yields obtained by the new methods represent the only information so far available. In other cases the new methods give results that have accuracy comparable to or better than those obtained by direct counting of neutrons. The data on neutron emission from fission can be greatly extended by these new methods if more fission mass yields are determined in the future.

Finally, suggestions are made as to the reason for the curious behavior of fission neutron emission as a function of fragment mass, and for other properties of fission.

II. DIRECT MEASUREMENTS OF NEUTRON YIELDS

The strong variation of neutron yield with fragment mass was first reported in 1954 by Fraser and Milton[1] for neutron fission of U^{233}. They counted fission neutrons in coincidence with fission fragment pulses from a double, gridded, collimated ionization chamber. Fragment masses were determined from the ratio of the two ion-chamber pulses, with corrections for energy loss. Each neutron was assumed to come from the fragment moving in the direction of the neutron counter, because of the strong correlation of neutron and fragment directions.[2]

The results obtained by Fraser and Milton are shown in Fig. 1, in which the fission neutron yield is given as a function of fragment mass. The average number of neutrons emitted by a light fragment of given mass is designated by ν_L, and ν_H similarly refers to the heavy fragment. The open circles show the total number ($\nu=\nu_L+\nu_H$) of neutrons emitted by both fragments, as a function of the mass of the heavy fragment.[3] Also shown are the yields of fragment masses (in percent per

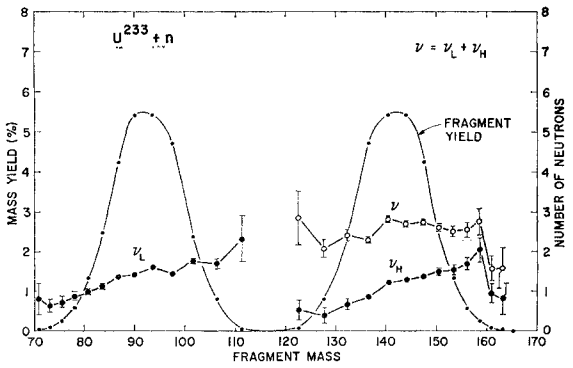

FIG. 1. Neutron and mass yields for fission of $U^{233}+n$(data of Fraser and Milton, uncorrected). Standard deviations are shown for the neutron yields in this and other figures.

* Work performed under the auspices of the U. S. Atomic Energy Commission. Several preliminary reports of this work have been given (references 47 and 48).

[1] J. S. Fraser and J. C. D. Milton, Phys. Rev. **93**, 818 (1954).

[2] J. S. Fraser, Phys. Rev. **88**, 536 (1952); also numerous more recent papers.

[3] The neutron data points for mass ratio 2.4 (masses 68.8 and 165.2), having very large standard deviations, have been omitted for clarity.

unit mass) as given by their ion chambers, uncorrected for the considerable experimental dispersion of mass.

It is apparent from Fig. 1 that most of the neutrons are emitted by the heavier light fragments and by the heavier heavy fragments, and that there is considerable slope to the fragment neutron yield (ν_L and ν_H) through each mass peak. The total neutron yield ν, however, shows much less dependence on mass ratio. These surprising results met with some skepticism at first, partly because of the uncertainty of the neutron efficiency correction. The two neutron counters, which were proton-recoil ion chambers, were strongly energy-dependent in efficiency. Furthermore, the neutron counting efficiency depends strongly on the angular correlation of the neutrons with fragment direction, an effect (see Appendix II) which varies with fragment mass and is very sensitive to the precise form of the center-of-mass emission spectrum.[4]

Fraser and Milton did not attempt to correct precisely for these variations of neutron counting efficiency, and no such attempt will be made here.[5] Hence, the neutron data (and the mass data) shown in Fig. 1 stand in need of various corrections. However, the sawtooth nature of the neutron yield for U^{233} fission, as reported by Fraser and Milton, has now been verified, as will be shown in a later section of this paper (see Fig. 7).

In 1959 Whetstone[6] reported the neutron emission from fission fragments of another nucleus, spontaneously fissioning Cf^{252}. His research used considerably improved equipment,[7] including a large liquid scintillator to detect neutrons, in coincidence with time-of-flight detectors for the two fission fragments. The fission foil was placed at the edge of the scintillator tank. The flat response of the liquid scintillator to neutrons of varying energy gave neutron data with accuracy considerably improved over the earlier work. The neutron efficiency correction involved only the angular correlation of neutrons and fragments, and used an evaporation-theory center-of-mass neutron spectrum.[4] In addition, Whetstone made a correction for the fraction of neutrons which were emitted into the laboratory hemisphere opposite to the direction of motion of the emitting fragment (see Appendix II).

Whetstone's Cf^{252} results, shown in Fig. 2, have a strong resemblance to the earlier results of Fraser and Milton for U^{233} (Fig. 1). Both sets of data, however, are in need of considerable correction for the effect of mass dispersion, which flattens and broadens each of the two segments (ν_L and ν_H) of the neutron yield curve (ν_f). Whetstone discussed this effect,[6] but did not correct for it, except in calculating average slopes.

However, it is possible to draw misleading conclusions from the published data as to the sharpness of the change in ν_f with mass near symmetrical fission. Hence, Whetstone's data have been corrected in this paper for the shift due to mass dispersion. This "dispersion shift" will be discussed in more detail below, as it is not usually taken into account. The results of this correction, using a mass dispersion given by $\sigma^2=15.9$, are shown in Fig. 3.

The dispersion correction applied here to Whetstone's data is based on the assumption that the true width of each peak of the initial Cf^{252} mass number distribution is given by the variance $\sigma^2=47.6$. This figure is based on an average of Whetstone's more recent unpublished mass data[8] and that of Milton and Fraser,[9] after each distribution has been corrected for the calculated experimental dispersion (see Appendix III), and for grouping of data.[10] The considerably larger width of Whetstone's published mass distribution[6] ($\sigma^2=63.5$, uncorrected, for each mass peak, including 0.44 due to grouping) is possibly due to an unexpectedly thick source foil; the measured energy distribution is consistent with this explanation.

Because of the considerable experimental mass dispersion in Whetstone's published data (amounting to the difference between 63.5 and 47.6, or $\sigma^2=15.9$), each neutron data point in Fig. 2 represents a weighted average of neutron yields over a considerable range of fragment masses. If the experimental dispersion is assumed to be Gaussian, it has a width at half-height equal to 9.4 mass units; if assumed rectangular, the over-all width is 13.8 mass units. In either case, each data point in Fig. 2 represents a weighted average over

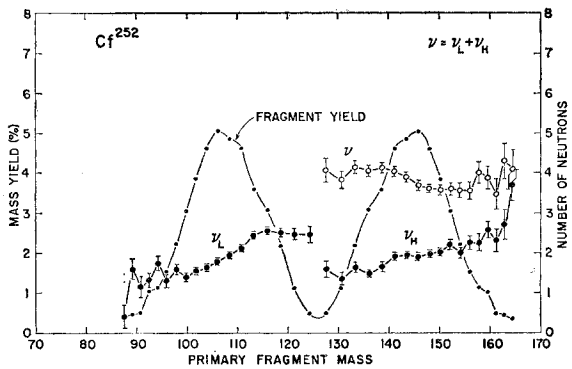

FIG. 2. Neutron and initial mass yields for fission of Cf^{252} (data of Whetstone, uncorrected).

[4] J. Terrell, Phys. Rev. **113**, 527 (1959).

[5] It appears, however, that a more precise efficiency correction for their data would give a ratio of average neutron numbers from light and heavy fragments much closer to 1.0 than the rough value of 1.24 reported in reference 1 (see Appendix II).

[6] S. L. Whetstone, Jr., Phys. Rev. **114**, 581 (1959).

[7] W. E. Stein and S. L. Whetstone, Jr., Phys. Rev. **110**, 476 (1958).

[8] S. L. Whetstone, Jr. (private communication).

[9] J. C. D. Milton and J. S. Fraser, Phys. Rev. **111**, 877 (1958).

[10] Sheppard's grouping correction is discussed in various textbooks, for example H. Cramèr, *Mathematical Methods of Statistics* (Princeton University Press, Princeton, New Jersey, 1946), pp. 359–363. When experimental data are presented as points, each covering a range h of the abscissa, a distribution is broadened thereby in variance by very nearly $h^2/12$. There are similar corrections for higher moments. These corrections are quite accurate for smoothly-varying distributions, and are correct on the average even for discontinuous distributions.

about 14 mass units, and is thus subject to a considerable "dispersion shift." Each data point is effectively moved away from its mass peak by this shift. The neutron data point plotted at mass 87.7, for instance, represents mostly fission fragments in the vicinity of mass 90 and above; the weighted average over the dispersion interval may be determined to be mass 91.1, and this is where the point should be plotted. This procedure has been carried out,[11] and the results are shown in Fig. 3. For points on the extreme edges of the two mass peaks the dispersion shift amounts to 3 or 4 mass units. A few of the original unshifted data points are shown (crosses) to indicate the extent of the dispersion shift.

In order to correct properly for dispersion shift it is necessary to obtain the undispersed mass distribution, also shown in Fig. 3. This was done by unfolding dispersion[12,12a] from an average of Whetstone's published mass distribution with the nearly identical, but statistically more reliable, mass data obtained from the same source by Stein and Whetstone[7] ($\sigma^2=61.5$, after grouping correction[10]).

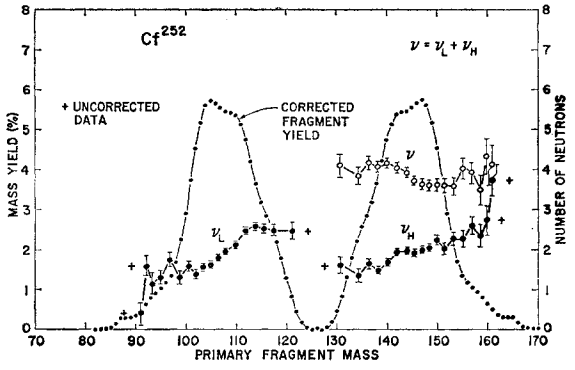

FIG. 3. Neutron and initial mass yields for fission of Cf^{252} (data of Whetstone, corrected for mass dispersion and dispersion shift of neutron data points). A few uncorrected data points are shown.

With the correction for dispersion shift, all of Whetstone's data points are shifted closer to the two peaks of mass yield, and the rate of change of ν_f with mass M is considerably increased through each peak. The average slopes $\langle d\nu_L/dM_L\rangle$ and $\langle d\nu_H/dM_H\rangle$ are increased by this correction in the ratio of uncorrected to corrected mass variance, a ratio of 1.33 in this case. No attempt has been made here to remove the added effect of experimental mass dispersion in smoothing the ν_f curve.

The most dramatic effect of removing dispersion shift is to increase the separation of data points near symmetric fission. Thus the near-discontinuity in ν_f seen in Fig. 2 is a more gradual change in Fig. 3. This effect is just opposite to the usual effect of removing dispersion (that of *increasing* slope) and is due to the fact that these points lie *between* the two mass peaks. Thus there is actually no sudden discontinuity of ν_f in Whetstone's data. There are, in fact, almost no Cf^{252} fissions occurring near symmetric mass division, for a range of 6 or 8 mass units. Hence data points taken in this region tend to be misleading, as they consist essentially only of fission events which occurred in adjacent mass regions.

Apalin *et al.*[13] have recently published fragment neutron data for neutron fission of U^{235}. Their neutron counter was a large liquid scintillation counter, with its desirable, relatively flat, response. They detected fission fragments with a double ionization chamber, similar to the type used by Fraser and Milton,[1] placed off to one side of the neutron detector. The use of a fission chamber necessarily added considerable width to the measured mass distribution, and caused corresponding dispersion shift in the neutron data points.

Apalin *et al.* corrected for angular correlation of neutrons and fragments, but used a fixed center-of-mass emission energy in their calculations. This automatically leads to the calculation of considerably less correlation, by about a factor of 2, than the more reasonable assump-

[11] Correction for dispersion shift could have been carried out most simply by assuming the undispersed mass distribution to be Gaussian in shape. For a Gaussian mass distribution of average mass $\bar{M}$ and rms width σ, and for a Gaussian experimental mass resolution of rms width σ_e, data taken in a mass interval centered at M represent the weighted average mass $M+(\bar{M}-M)\sigma_e^2/(\sigma^2+\sigma_e^2)$. Thus the dispersion shift is linear with mass in this simple case. More generally, the dispersion shift in mass is given to first order by $-\sigma_e^2(dY/dM)/Y$, in which $Y(M)$ is the true yield of mass M and is considered to be a continuous function. The best correction for dispersion shift, for non-Gaussian cases, is obtained by folding an assumed experimental dispersion distribution into the undispersed mass distribution, to obtain a weighted average mass for each experimental mass interval used; this was the method actually used in this work. The results have been found not to be sensitive to the exact shape of the dispersion function used, and a rectangular distribution was used for simplicity.

[12] Removal of dispersion from mass yield data may be quite easily done by folding into the data a distribution function having negative second central moment. An example of such an undispersing distribution function is -1, $+3$, -1, for masses $M-1$, M, $M+1$. This is symmetrical and normalized (the sum is 1.0), and has a second central moment of -2. When folded into an experimental mass distribution, it will reduce its variance by precisely 2 units. It is easy to construct such distributions having any desired negative variance and number of points. It can be shown that, if a continuous distribution is representable by a power series of no more than cubic order over a range R greater than the full extent of the (symmetrical) dispersion function, any symmetrical undispersing function of the proper variance, if used within the range R, will recover the original function. For reasonably smooth experimental distributions the exact forms of the dispersing and undispersing functions are thus not of great significance. This unfolding or dispersion-removal process tends to exaggerate slight statistical point-to-point fluctuations normally present in a distribution. When considerable dispersion is being removed this can make accidental molehills look like mountains. In such a case it is better to smooth the experimental distribution before undispersing it. One good method of smoothing is to combine adjacent data points. This, of course, slightly widens the distribution, and the necessary grouping correction (reference 10) must be allowed for in the removal of dispersion.

[12a] *Note added in proof.* This operational method of inverting the folding operation can be made to correct the central moments properly to as high an order as desired. For example, a five-element undispersing function should have $\mu_4=G\sigma^4-\mu_4^*$, where σ^2 and μ_4^* are the moments of the dispersion function; this operator will correct properly a fifth-order polynomial.

[13] V. F. Apalin, Yu. P. Dobrynin, V. P. Zakharova, I. E. Kutikov, and L. A. Mikaelyan, Atomnaya Energ. **8**, 15 (1960) [translation: Soviet J. Atomic Energy **8**, 10 (1961)].

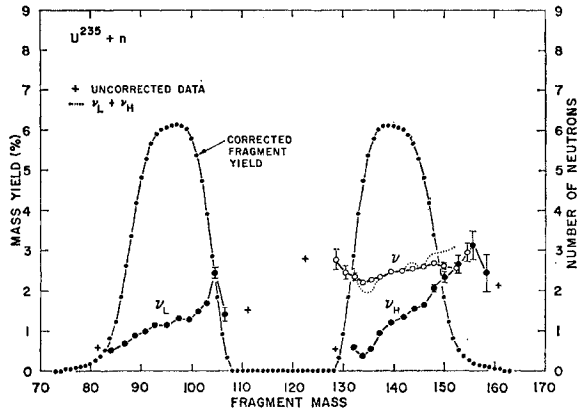

FIG. 4. Neutron and mass yields for fission of $U^{235}+n$ (single-fragment data of Apalin *et al.*, corrected for mass dispersion and dispersion shift of neutron data points, and partially recorrected for neutron efficiency). The sum of ν_L and ν_H is shown as a dotted line. Their independently-measured fragment-pair data on ν are shown as open circles. A few uncorrected data points are shown.

tion[4] of a wide spectrum of center-of-mass neutron energies. Apparently they also did not correct for neutrons emitted and detected backward from fragments. Their published data[13] have been corrected here for dispersion shift,[11,12,14] and an attempt has been made to make a better correction for neutron angular correlation (see Appendix II); the results are shown in Fig. 4. As in Fig. 3, there are also shown in Fig. 4 a few of the original, unshifted, data points (crosses), to indicate the extent of the dispersion shift correction, and also, in this case, of the recorrection for neutron counting efficiency.

Two sets of data are shown for the total neutron emission ν from both fragments. One set (the dotted line) is simply the sum, $\nu_L+\nu_H$, of the results shown for light and heavy fragments. This set of data is not shown as individual points because the light and heavy fragment data do not correspond to the same mass ratios, and hence, cannot be added point by point. The other set of data on ν (fragment-pair data, open circles) is perhaps more reliable, and was measured directly by placing the fission chamber in the center of the liquid scintillator (4π geometry) instead of off to one side. Hence these points are not greatly affected by angular correlation of neutrons, and only dispersion shift has been corrected for here.

[14] The dispersion shift correction to the data of Apalin *et al.* made use of the corrected single-fragment mass yield curve shown in Fig. 4. This was obtained by unfolding experimental dispersion of $\sigma^2=8.8$ (equivalent to a rectangular distribution of total width 10.3 mass units) from the published mass distribution curve for data on ν_L and ν_H, slightly smoothed. This dispersion correction is based on the difference between the variance of the published mass distribution ($\sigma^2=39.6$, including 0.6 for grouping) and that of the mass yields given by time-of-flight data (30.8, after correction; see Table I). The dispersion shift correction for ν_L and ν_H data points amounts to a maximum of 3 or 4 mass units. For the independently measured fragment-pair data on ν the shift is larger, as much as 5 or 6 mass units, because of the greater width of the associated mass data (variance $\sigma^2=42.4$, needing reduction by 11.6).

The approximate recorrection for neutron angular correlation (see Appendix II) makes a considerable difference in the data for ν_f, as may be seen in Fig. 4. Proper allowance for an emission spectrum instead of a fixed energy leads here to lower values of ν_L and higher values of ν_H, by 5 or 10%; the biggest change is for the highest mass ratios. The recorrected values lead to the result $\bar{\nu}_L \cong \bar{\nu}_H$.

As seen in Fig. 4, Apalin's corrected data are rather similar to that previously discussed for U^{233} (Fig. 1) and Cf^{252} (Fig. 3). No neutron data exist for a considerable range of masses near symmetry, amounting to perhaps 20 mass units in this case, primarily because almost no fissions occur in this range. As pointed out by Apalin *et al.*,[13] the behavior of $\nu_f(M)$ is not well-defined in this region.

In addition to the data on ν_f which have been described above,[1,6,13] there are also three published sets of data on the total neutron number ν (but not ν_f) for Cf^{252}, as a function of fragment mass.[7,15,16] Such data on ν alone are easier to obtain accurately, and are subject to much less uncertainty in the necessary corrections, than data on ν_f. The data on ν, based on 4π counting, need primarily only correction for dispersion shift, and agree reasonably well with the Cf^{252} data in Fig. 3.

III. NEUTRON YIELDS FROM MOMENTS OF FRAGMENT MASS DISTRIBUTIONS

It is possible to obtain excellent independent data on $\nu_f(M)$ from essentially nothing more than data on the yield of fragment masses, by the new methods to be reported in this paper. What is basically necessary is the combination of data on initial and final fragment masses (before and after emission of neutrons). Radiochemical and mass-spectrometric methods have given much accurate data on the yields of *final* fragment masses. Recent time-of-flight methods now give data on *initial* mass yields which are almost comparable in accuracy, after correction for experimental mass resolution. The information which may be obtained from the first and second moments of these mass distributions is discussed in this section.

A. Historical

It has been a common practice to estimate $\bar{\nu}$ from the average final fission product mass numbers, $\bar{L}$ and $\bar{H}$ (for light and heavy groups of the final fragments), by means of the equation

$$\bar{\nu}=A-\bar{L}+\bar{H}. \tag{1}$$

Where radiochemical data are scarce, the reflection of yields about a mirror point of mass has been used to estimate $\bar{\nu}$.

[15] D. A. Hicks, J. Ise, Jr., R. V. Pyle, G. Choppin, and B. Harvey, Phys. Rev. **105**, 1507 (1957).

[16] H. R. Bowman and S. G. Thompson, *Proceedings of the Second United Nations International Conference on the Peaceful Uses of Atomic Energy, Geneva, 1958* (United Nations, Geneva, 1958), Vol. 15, p. 212.

TABLE I. Fission mass data and neutron yields. The symbols M_L and M_H represent the initial mass numbers of light and heavy fission fragments (before neutron emission); similarly, L and H refer to final fragment mass numbers. The numbers of neutrons emitted by light and heavy fragments are denoted by ν_L and ν_H; the sum of these for a given mass ratio is ν. The symbol $\nu_f(M)$ denotes both $\nu_L(M_L)$ and $\nu_H(M_H)$. Averages are indicated by bars or angular brackets. Estimated standard deviations are given for all quantities.

	$U^{233}+n$	$U^{235}+n$	$Pu^{239}+n$	Cf^{252}
$\bar{M}_L$	94.42±0.10[a]	96.01±0.10[a]	100.35±0.12[a]	108.2 ±0.4[b]
$\bar{M}_H$	139.58±0.10[a]	139.99±0.10[a]	139.65±0.12[a]	143.8 ±0.4[b]
$\bar{L}$	93.16±0.15[c]	94.89±0.07[c]	98.95±0.10[c]	106.1 ±0.3[d]
$\bar{H}$	138.39±0.15[c]	138.68±0.07[c]	138.24±0.10[c]	142.0 ±0.3[d]
$\bar{\nu}_L=\bar{M}_L-\bar{L}$	1.26±0.18	1.12±0.12	1.40±0.14	2.1 ±0.5
$\bar{\nu}_H=\bar{M}_H-\bar{H}$	1.19±0.18	1.31±0.12	1.41±0.14	1.8 ±0.5
$\bar{\nu}=A-\bar{L}-\bar{H}$	2.45±0.21	2.43±0.10	2.81±0.14	3.9 ±0.4
$\bar{\nu}$(direct)	2.50±0.02[e]	2.43±0.02[e]	2.89±0.03[e]	3.79 ±0.04[f]
$\sigma^2(\nu)$	1.16±0.08[g]	1.22±0.04[g]	1.38±0.14[g]	1.54 ±0.04[g]
$\sigma^2(M_L)=\sigma^2(M_H)$	32.7 ±2[a]	30.8 ±2[a]	38.9 ±2[a]	47.6 ±4[b]
$\sigma^2(L)$	28.3 ±1[c]	27.1 ±1[c]	34.5 ±1[c]	39.0 ±2[d]
$\sigma^2(H)$	26.4 ±1[c]	27.1 ±1[c]	31.3 ±1[c]	40.1 ±2[d]
$\langle\sigma^2(\nu_f;M)\rangle$[h,i]	0.56±0.3	0.61±0.3	0.66±0.3	0.76 ±0.4
$\langle d\nu_L/dM_L\rangle$(indirect)[i]	0.08±0.03	0.07±0.03	0.07±0.03	0.10 ±0.05
$\langle d\nu_H/dM_H\rangle$(indirect)[i]	0.11±0.03	0.07±0.03	0.11±0.03	0.09 ±0.05
$\langle d\nu/dM_H\rangle$(indirect)[i]	0.03±0.02	0.00±0.02	0.04±0.02	−0.01 ±0.03
$\langle d\nu_L/dM_L\rangle$(direct)[j]	0.04±0.03[k]	0.05±0.03[l]	···	0.06 ±0.03[m]
$\langle d\nu_H/dM_H\rangle$(direct)[j]	0.06±0.03[k]	0.10±0.03[l]	···	0.04 ±0.03[m]
$\langle d\nu/dM_H\rangle$(direct)[j]	0.02±0.03[k]	0.02±0.02[n]	···	−0.013±0.01[o]

[a] Average of time-of-flight data of Stein (reference 21) and of Milton and Fraser (reference 22).
[b] Average of time-of-flight data of Whetstone (reference 8) and of Milton and Fraser (reference 9).
[c] Calculated from summary and interpolation of Walker (reference 28).
[d] Based on data of Nervik (reference 29), Glendenin and Steinberg (reference 31), and of Cuninghame (reference 30), plus interpolated and extrapolated yields.
[e] World weighted averages (reference 32).
[f] Asplund *et al.* (reference 33).
[g] As summarized by Terrell (reference 37).
[h] Standard deviation allows for lack of information as to correlation between ν_L and ν_H for given mass ratio.
[i] Calculated from mass-yield data given above, using Eqs. (31) to (33).
[j] Linear regression slopes corrected for mass dispersion, based on neutron counting data and Eqs. (16), (17), and (22).
[k] Based on data of Fraser and Milton (reference 1), which need a better efficiency correction; this would probably increase all the slopes.
[l] Based on data of Apalin *et al.* (reference 13), after partial recorrection for efficiency. The values of $\langle d\nu_L/dM_L\rangle$ and $\langle d\nu^M/dM_H\rangle$ based directly on the published data are 0.04 and 0.08, respectively.
[m] Based on data of Whetstone (reference 6).
[n] Based on fragment pair data of Apalin *et al.* (reference 13). The value based on partially corrected single-fragment data is 0.05, and on data as published is 0.04.
[o] Based on data of Stein and Whetstone (reference 7). The value based on data of Whetstone (reference 6) is −0.022.

However, much more information than this can be obtained from the mass yields. The possibility of this was pointed out in 1954 by Steinberg and Glendenin,[17] who deduced that ν near symmetric fission is smaller than the overall average $\bar{\nu}$, for the cases of Cm^{242} and $U^{235}+n$. Their conclusion was based on the method of summing complementary masses, that is, masses on corresponding sides of light and heavy peaks which have the same final yield. Such methods have become the standard means used by radiochemists to determine $\bar{\nu}$, and in a few cases[17–20] some information on $\nu(M_H)$.

Unfortunately, the reflection or matching of individual mass yields is inherently not an accurate procedure, and leads to unavoidable systematic errors in ν, even with perfect data. Furthermore, it cannot be used to determine ν in the vicinity of the fission fragment mass peaks, nor in the valley between. This usual method is possible only where yields change rapidly with mass, on the sides of the peaks, and is subject even there to systematic error in ν amounting to 0.1, 0.2, or more. As to the yields (ν_f) from individual fragments, the use of radiochemical data alone gives no information at all. Methods for obtaining better information on neutron yields will be given below.

B. Use of Average Masses (First Moments)

The simplest combination of data on initial and final fission fragment mass yields, using only the average masses of the light and heavy fragments before and after neutron emission, gives average values $\bar{\nu}_L$ and $\bar{\nu}_H$. The necessary equations, based on the assumption that all of the neutrons are emitted by the fragments, are

$$\bar{\nu}_L=\bar{M}_L-\bar{L}, \tag{2}$$

$$\bar{\nu}_H=\bar{M}_H-\bar{H}. \tag{3}$$

Here M_L and M_H denote the initial mass numbers of light and heavy fragments ($M_L+M_H=A$). To use this

[17] E. P. Steinberg and L. E. Glendenin, Phys. Rev. **95**, 431 (1954).
[18] T. T. Sugihara, P. J. Drevinsky, E. J. Troianello, and J. M. Alexander, Phys. Rev. **108**, 1264 (1957).
[19] R. B. Duffield, R. A. Schmitt, and R. A. Sharp, *Proceedings of the Second United Nations International Conference on the Peaceful Uses of Atomic Energy, Geneva, 1958* (United Nations, Geneva, 1958), Vol. 15, p. 202.
[20] Yu. A. Zysin, A. A. Lbov, and L. I. Sel'chenkov, Atomnaya Energ. **8**, 409 (1960) [translation: Soviet J. Atomic Energy **8**, 343 (1961)].

method it is necessary that the two fission fragment peaks be reasonably well separated, so that the light and heavy fragment mass data overlap only slightly, if at all. This is usually the case for low-energy fission and time-of-flight equipment. As was pointed out first by Stein,[21] the average fragment velocity for a given mass is changed only trivially by isotropic emission of neutrons. There is a larger effect, however, on the width of the velocity distribution and hence on the apparent distribution of final fragment masses as determined from the ratio of two velocities[6,7,9,21] (see Appendix III).

This method [Eqs. (2) and (3)] has recently been used by Milton[22] to determine $\bar{\nu}_L$ and $\bar{\nu}_H$. The results of such computations, with results similar to Milton's, are presented in the upper half of Table I. The data in this table are for those fissioning nuclides for which there are now sufficiently good data on both initial and final mass yields—thermal neutron fission of U^{233}, U^{235}, and Pu^{239}, and spontaneous fission of Cf^{252}.

The average initial masses of light and heavy fragments ($\bar{M}_L$ and $\bar{M}_H$) have been determined in each case from the average of two independent sets of double-velocity time-of-flight data, taken at Chalk River by Milton and Fraser,[9,22] and at Los Alamos by Stein and Whetstone.[8,21] It is necessary to take data on about 4000 fissions in order to determine the average masses $\bar{M}_L$ and $\bar{M}_H$ to an rms error of 0.1 mass unit,[23,23a] if background effects, systematic errors, and other troubles, are not too important. This criterion is nearly met by 2 out of 3 of Stein's sets of data[21] (with the exception of Pu^{239}, for which only 680 fissions were observed), and is greatly exceeded in the other sets of data.[8,9,22] There is excellent agreement between the two sets of data as to the average initial masses in three of the cases (the maximum difference being 0.14, for U^{235}), but for Cf^{252} there is a significant discrepancy. Here Whetstone's data yield $\bar{M}_L=107.83\pm0.03$, whereas the data of Milton and Fraser give 106.61 ± 0.02 (the standard deviations are based only on counting statistics). Because of the possibility of systematic errors due to, for instance, unevenly thick foils, the average masses $\bar{M}_L$ and $\bar{M}_H$ shown in Table I have been determined by an equally-weighted average of the two sets of data in each case.

Several excellent compilations of radiochemical and mass spectrometric data on final mass yields have been published; the most recent of these are by Katcoff,[24,25] Tomlinson and his co-workers,[26,27] Walker,[28] and Nervik.[29] All of these compilations were used in the course of the work reported here, in addition to others made independently for this paper; the differences in results were not significant. However, it was decided to publish only those results based on Walker's compilation, for the three cases of neutron-induced fission, since his report gives a complete set of mass yields, with interpolation and extrapolation where necessary.

No such complete compilation (with interpolation) of final mass yields has been published for Cf^{252} fission, so that it was necessary to construct one for the purposes of this paper. The comprehensive work of Nervik and his co-workers[29] was taken as the primary basis of the adopted set of mass yields, with some additions from the work of Cuninghame,[30] and of Glendenin and Steinberg.[31] The measured yield values are shown in a later section of this paper for this case, and also for the other three cases (Figs. 5–10).

The standard deviations given in Table I for these values of $\bar{L}$, $\bar{H}$, and $\bar{\nu}$ calculated from final mass yields are based on estimations of the errors in these yields. An rms uncertainty of 0.1 in the average mass number $\bar{L}$ (or $\bar{H}$) will be produced by a set of final mass yields similar in accuracy to that produced statistically by 4000 fissions.[23] This corresponds to 6% relative uncertainty in mass yields of 6% or 7%, about 16% uncertainty for mass yields at the 1% level, and 50% uncertainty in 0.1% yields. The smaller yields are not nearly this poorly known where measured, but there are gaps which must be filled by interpolation. The values of $\bar{\nu}$ determined from the radiochemical and mass-spectrometric data are in excellent agreement with those more directly measured.[32,33] However, these may not be completely independent estimates.

It may be seen in Table I that there is evidence of approximately equal neutron emission from light and heavy fragments ($\bar{\nu}_L \cong \bar{\nu}_H$). This is in contrast to conclusions reached in several other papers, which are discussed in Appendix II.

C. Use of Second Moments of Mass Distributions

The average slopes $\langle d\nu_L/dM_L\rangle$ and $\langle d\nu_H/dM_H\rangle$ may also be determined directly from mass yield data, by a slightly more complete use of the data. These slopes are

[21] W. E. Stein, Phys. Rev. **108**, 94 (1957).
[22] J. C. D. Milton, Bull. Am. Phys. Soc. **6**, 16 (1961).
[23] For a distribution of masses with experimental second central moment σ^2 (which is 30 or 40 for light fission fragments, or heavy fragments), the rms error in the average mass as determined by N observations is $\sigma/\sqrt{N}$.
[23a] *Note added in proof.* Whetstone's most recent Cf^{252} data (private communication) yield $\bar{M}_L=108.29\pm0.05$ and $\sigma^2(M_L)$ 46 ± 1, agreeing well with the averages in Table I.
[24] S. Katcoff, Nucleonics **16**, No. 4, 78 (1958).
[25] S. Katcoff, Nucleonics **18**, No. 11, 201 (1960).
[26] H. R. Fickel and R. H. Tomlinson, Can. J. Phys. **37**, 916, 926 (1959).
[27] D. R. Bidinosti, D. E. Irish, and R. H. Tomlinson, Can. J. Chem. **39**, 628 (1961).
[28] W. H. Walker, Chalk River Report CRRP-913, Atomic Energy of Canada Limited, Chalk River, Ontario, 1960 (unpublished).
[29] W. E. Nervik, Phys. Rev. **119**, 1685 (1960).
[30] J. G. Cuninghame, J. Inorg. & Nuclear Chem. **6**, 181 (1959).
[31] L. E. Glendenin and E. P. Steinberg, J. Inorg. & Nuclear Chem. **1**, 45 (1955).
[32] D. J. Hughes, B. A. Magurno, and M. K. Brussel, *Neutron Cross Sections*, Brookhaven National Laboratory Report BNL-325 (U. S. Government Printing Office, Washington, D. C., 1960), 2nd ed., Suppl. No. 1.
[33] I. Asplund, H. Condé, and N. Starfelt, Försvarets Forskningsanstalt Report FOA 4, A4200-411, 1961 (unpublished).

related to the widths of the various mass peaks—light and heavy, initial and final.

The necessary equations may be derived from the fundamental relations between initial fragment mass numbers M_L and M_H, final mass numbers L and H, and numbers of neutrons emitted from light and heavy fragments, ν_L and ν_H:

$$M_L+M_H=A, \tag{4}$$

$$L+H+\nu=A, \tag{5}$$

$$\nu_L+\nu_H=\nu, \tag{6}$$

$$L+\nu_L=M_L, \tag{7}$$

$$H+\nu_H=M_H. \tag{8}$$

In these equations A is the mass number of the fissioning compound nuclide, and ν is the total number of neutrons emitted in a single fission event. All of the quantities in these equations are integers, and refer to a single fission event. Averaging these equations over all fission events occurring for a given compound nuclide leads obviously to five more equations, of which three examples have already been given in Eqs. (1) to (3).

From Eqs. (4) to (8) it is easy to derive a large number of relations between variances and covariances of M_L, M_H, L, H, ν_H, ν_L, and ν, simply by squaring both sides of any given equation and averaging over all modes of fission. Since we are concerned with the correlation of initial fragment mass with neutron emission, the following simple relations are useful:

$$\sigma^2(M_L)=\sigma^2(M_H), \tag{9}$$

$$C(\nu_L,M_L)=\tfrac{1}{2}[\sigma^2(M_L)+\sigma^2(\nu_L)-\sigma^2(L)], \tag{10}$$

$$C(\nu_H,M_H)=\tfrac{1}{2}[\sigma^2(M_H)+\sigma^2(\nu_H)-\sigma^2(H)], \tag{11}$$

$$C(\nu_L,\nu_H)=\tfrac{1}{2}[\sigma^2(\nu)-\sigma^2(\nu_L)-\sigma^2(\nu_H)], \tag{12}$$

$$C(\nu_L,\nu_H;M_H)=\tfrac{1}{2}[\sigma^2(\nu;M_H)-\sigma^2(\nu_L;M_L)-\sigma^2(\nu_H;M_H)]. \tag{13}$$

In all of these equations the symbol $\sigma^2(x)$ refers to the second central moment, or variance,

$$\sigma^2(x)\equiv\langle x^2\rangle-\bar{x}^2, \tag{14}$$

while $C(x,y)$ is the covariance of the variables x and y:

$$C(x,y)\equiv\langle xy\rangle-\bar{x}\bar{y}. \tag{15}$$

If x and y are independent quantities, completely uncorrelated, their covariance is zero.[34] The conditional covariance $C(\nu_L,\nu_H;M_H)$ is defined as the covariance of ν_L and ν_H for fixed M_H (or M_L). Obviously this equation is obtained by averaging over only a portion of all fission modes. Here, and elsewhere in this paper, averages are denoted either by bars or by angular brackets.

From Eq. (9), the variances of the light and heavy initial mass distributions are equal, so that they may be used interchangeably in these equations. It is obvious that the relations developed in this section are usable only when light and heavy mass peaks are clearly separable, as is usually the case for low-energy fission; more general relations will be derived in Sec. IV.

All of the variances in Eqs. (9) to (13) are experimentally measurable, in principle, so that it would be simple to evaluate all the covariances directly from these equations if all the necessary experiments had been done. However, it is not difficult to obtain considerable information from data available now. The missing information primarily has to do with the small variances of ν_L and ν_H.

The average slopes $\langle d\nu_L/dM_L\rangle$ and $\langle d\nu_H/dM_H\rangle$ are directly connected with the covariances in Eqs. (10) and (11) by a general theorem,[34] which gives the equations

$$C(\nu_L,M_L)=\langle d\nu/dM_L\rangle\sigma^2(M_L), \tag{16}$$

$$C(\nu_H,M_H)=\langle d\nu_H/dM_H\rangle\sigma^2(M_H). \tag{17}$$

The "average slopes" are more precisely defined as the slopes of the weighted least-square fits of linear regression curves to the data on $\nu_L(M_L)$ and $\nu_H(M_H)$. Here, and elsewhere in this paper, $\nu_L(M_L)$ should be understood to mean $\langle\nu_L;M_L\rangle$, which is the (conditional) average value of ν_L for given M_L. A similar meaning should be attached to $\nu_H(M_H)$, and to the more general notation $\nu_f(M)$, which refers to both light and heavy mass peaks.

The regression lines which are to be fitted to the data have the form

$$\nu_L(M_L)\equiv\langle\nu_L;M_L\rangle=\bar{\nu}_L+\langle d\nu_L/dM_L\rangle(M_L-\bar{M}_L), \tag{18}$$

$$\nu_H(M_H)\equiv\langle\nu_H;M_H\rangle=\bar{\nu}_H+\langle d\nu_H/dM_H\rangle(M_H-\bar{M}_H). \tag{19}$$

The least-square fit which is necessary for Eqs. (16) and (17) to be correct[34] is weighted only by the initial fission mass yields. Fortunately, this weighting is ordinarily close to the more usual weighting based on the statistical uncertainties of the data points $\nu_L(M_L)$ and $\nu_H(M_H)$. It should be clearly understood that, with this definition of average slope, Eqs. (16) and (17) are quite general, and do not involve any assumptions as to the distributions of M_L, M_H, ν_L, or ν_H. In particular, no assumption is necessary that the neutron yield points are actually linear with mass; Eqs. (18) and (19) merely represent the best linear fits to the data.

The general relations in Eqs. (16) and (17), when combined with the equally general Eqs. (10) and (11), give

$$\langle d\nu_L/dM_L\rangle=[\sigma^2(M_L)+\sigma^2(\nu_L)-\sigma^2(L)]/2\sigma^2(M_L), \tag{20}$$

$$\langle d\nu_H/dM_H\rangle=[\sigma^2(M_H)+\sigma^2(\nu_H)-\sigma^2(H)]/2\sigma^2(M_H). \tag{21}$$

The average rate of change of $\nu=\nu_L+\nu_H$ with, for example, M_H, may be determined from these equations and the relation

$$\langle d\nu/dM_H\rangle=\langle d\nu_H/dM_H\rangle-\langle d\nu_L/dM_L\rangle. \tag{22}$$

[34] H. Cramèr, *Mathematical Methods of Statistics* (Princeton University Press, Princeton, New Jersey, 1946), or any of a number of other texts on statistics.

Thus all of these average slopes may be determined directly from mass-yield data alone, except for the need of data on the small variances $\sigma^2(\nu_L)$ and $\sigma^2(\nu_H)$. No assumptions have been made in deriving Eqs. (20) and (21), except as to separability of light and heavy mass peaks, and emission of the neutrons by the fragments.

The major effects of fragment neutron emission on mass distribution may be understood from Eqs. (20) and (21). If neutron emission were constant with fragment mass, so that $\langle d\nu_L/dM_L\rangle=\langle d\nu_H/dM_H\rangle=0$, emission would make each peak of the final mass distribution slightly broader than that of the initial distribution; the variance $\sigma^2(L)$, for instance, would be equal to the sum of the variances $\sigma^2(\nu_L)$ and $\sigma^2(M_L)$. The fact that $\nu_L(M_L)$ actually changes considerably with mass makes a difference in this situation; with the lightest of the light fragments emitting almost no neutrons, this side of the light mass peak is not shifted by emission nearly as much (to lower masses) as is the heavy side of the light mass peak. Hence this correlation of neutron emission and fragment mass makes the final distribution of light fragment masses narrower than the initial distribution, and this is also true of the heavy peak. Thus the extent to which each peak of the final (radiochemical) mass distribution is narrower than the initial (time-of-flight) distribution is a measure of the slopes $\langle d\nu_L/dM_L\rangle$ and $\langle d\nu_H/dM_H\rangle$. It also follows from Eqs. (20) to (22) that if $\langle d\nu/dM_H\rangle$ is positive, the rms width of the light final mass peak must be greater than that of the heavy final mass peak,[35] assuming $\sigma^2(\nu_L)\cong\sigma^2(\nu_H)$.

All of the variances of mass distributions which appear on the right sides of Eqs. (20) and (21) can be determined from experimental data, and are given in the lower half of Table I for the usual four cases. The estimated standard deviations are based on the uncertainties of the individual mass yields, and also, for the initial mass data, on the possibility of systematic errors in measuring fragment flight-times and correcting for experimental mass resolution. This last correction reduces $\sigma^2(M_L)$ by about 1.0 in the case of good time-of-flight data (see Appendix III).

When fission events are analyzed one by one, as in the time-of-flight experiments, it may be shown from statistical considerations[36] that only about 2000 fission events are needed to define $\sigma^2(M_L)$ to an rms uncertainty of ±1. However, this is smaller than the standard deviations given in Table I for $\sigma^2(M_L)$. Most of the uncertainty in this variance is due to possibilities of systematic error. The two sets of data on neutron-induced fission give values of $\sigma^2(M_L)$ differing from each other, after resolution correction, by 1.2 to 3.5. There is a more serious discrepancy for Cf^{252} fission, for which the corrected data of Milton and Fraser[9] give $\sigma^2(M_L)=43.5$, while Whetstone's data[8,23a] yield $\sigma^2(M_L)=51.3$. The figures for $\sigma^2(M_L)$ given in Table I are based in each case on an equally-weighted average of the two mass distributions.

The standard deviations of $\sigma^2(L)$ and $\sigma^2(H)$ were estimated from the radiochemical and mass-spectrometric data by the use of similar considerations, except that systematic errors play a smaller part. Part of the uncertainty here comes from missing yields, which must be interpolated or extrapolated. This is particularly the case for Cf^{252}.

Equations (20) and (21) require also knowledge of the variances $\sigma^2(\nu_L)$ and $\sigma^2(\nu_H)$. No direct experimental data on these quantities have been published. Since $\sigma^2(\nu)$ is well determined experimentally[37,38] (see Table I), it is possible to obtain values of $\sigma^2(\nu_L)$ and $\sigma^2(\nu_H)$ from Eq. (12) by making reasonable physical assumptions.

The physical assumptions are most reasonably made with respect to variances and covariances for given fragment mass, i.e., conditional variances and covariances. The assumption of linear regression [Eqs. (18) and (19)], which is a fairly good approximation to the results discussed in this paper, leads to simple relations between over-all and conditional variances and covariances:

$$\sigma^2(\nu_L)=\langle d\nu_L/dM_L\rangle^2\sigma^2(M_L)+\langle\sigma^2(\nu_L;M_L)\rangle, \tag{23}$$

$$\sigma^2(\nu_H)=\langle d\nu_H/dM_H\rangle^2\sigma^2(M_H)+\langle\sigma^2(\nu_H;M_H)\rangle, \tag{24}$$

$$C(\nu_L,\nu_H)=-\langle d\nu_L/dM_L\rangle\langle d\nu_H/dM_H\rangle\sigma^2(M_H)+\langle C(\nu_L,\nu_H;M_H)\rangle. \tag{25}$$

These approximate relations may be substituted into the exact Eqs. (12), (20), and (21) to give

$$[\langle d\nu_H/dM_H\rangle-\langle d\nu_L/dM_L\rangle]^2=[\sigma^2(\nu)-\langle\sigma^2(\nu_L;M_L)\rangle-\langle\sigma^2(\nu_H;M_H)\rangle-2\langle C(\nu_L,\nu_H;M_H)\rangle]/\sigma^2(M_H), \tag{26}$$

$$[1-\langle d\nu_L/dM_L\rangle]^2=[\sigma^2(L)-\langle\sigma^2(\nu_L;M_L)\rangle]/\sigma^2(M_H), \tag{27}$$

$$[1-\langle d\nu_H/dM_H\rangle]^2=[\sigma^2(H)-\langle\sigma^2(\nu_H;M_H)\rangle]/\sigma^2(M_H). \tag{28}$$

These three equations contain five unknowns:

$$\langle d\nu_L/dM_L\rangle,\ \langle d\nu_H/dM_H\rangle,\ \langle\sigma^2(\nu_L;M_L)\rangle,\ \langle\sigma^2(\nu_H;M_H)\rangle,$$

and

$$\langle C(\nu_L,\nu_H;M_H)\rangle.$$

In order to solve the equations, it is necessary to assume two more relations. Perhaps the most reasonable

[35] G. P. Ford (private communication) has previously derived this relation. It was used, at least implicitly, in several earlier papers (references 17 to 20).

[36] For a distribution of masses with experimental second and fourth central moments σ^2 and $k\sigma^4$, the rms error in the variance σ^2, as determined by N mass observations, is very nearly $\sigma^2[(k-1)/N]^{\frac{1}{2}}$. For a Gaussian distribution k is precisely 3, but for light fission fragments it is about 2.5, while $\sigma^2(M_L)$ is about 30 or 40.

[37] J. Terrell, Phys. Rev. **108**, 783 (1957).

[38] Note that $\sigma^2(\nu)\cong1.25$ is larger than the square of the standard deviation characterizing the fragment excitation energy, $\sigma=1.08$, as discussed in reference 37. The difference is due to Sheppard's correction (reference 10) and amounts to 1/12.

assumptions are:

$$\langle\sigma^2(\nu_L;M_L)\rangle=\langle\sigma^2(\nu_H;M_H)\rangle=\langle\sigma^2(\nu_f;M)\rangle, \quad (29)$$

$$\langle C(\nu_L,\nu_H;M_H)\rangle=0. \quad (30)$$

Equation (29) essentially amounts to the assumption that light and heavy fragments have similar distributions of excitation energy. Equation (30) would follow from the assumption that excitation energies of light and heavy fragments are completely uncorrelated, for a given mass ratio. Both Eqs. (29) and (30) are probably the most reasonable assumptions to make[37,39] in the absence of information on these matters. Of course it would be much better to have experimental information on $\sigma^2(\nu_L;M_L)$, $\sigma^2(\nu_H;M_H)$, and $C(\nu_L,\nu_H;M_H)$, as these factors are of fundamental importance to fission theory. All of these quantities are experimentally accessible in principle, and in addition are related by Eq. (13).

With the assumption of Eqs. (29) and (30), Eqs. (26) to (28) may now be solved simultaneously, giving

$$[1-\langle d\nu_L/dM_L\rangle]^2=(\alpha^2+\beta^2)^{\frac{1}{2}} +\alpha\cong[\sigma^2(L)-\tfrac{1}{2}\sigma^2(\nu)]/\sigma^2(M_H), \quad (31)$$

$$[1-\langle d\nu_H/dM_H\rangle]^2=(\alpha^2+\beta^2)^{\frac{1}{2}} -\alpha\cong[\sigma^2(H)-\tfrac{1}{2}\sigma^2(\nu)]/\sigma^2(M_H), \quad (32)$$

$$\langle\sigma^2(\nu_f;M)\rangle=\tfrac{1}{2}\sigma^2(\nu)-\tfrac{1}{2}\sigma^2(M_H)\langle d\nu/dM_H\rangle^2, \quad (33)$$

in which

$$\alpha\equiv[\sigma^2(L)-\sigma^2(H)]/2\sigma^2(M_H) \quad (34)$$

and

$$\beta\equiv[\sigma^2(L)+\sigma^2(H)-\sigma^2(\nu)]/2\sigma^2(M_H). \quad (35)$$

The approximations in Eqs. (31) and (32) are based on $|\alpha|\ll\beta$.

By means of Eqs. (31) to (33), the fission-fragment mass-yield widths summarized in Table I may be used to calculate $\langle d\nu_L/dM_L\rangle$, $\langle d\nu_H/dM_H\rangle$, $\langle d\nu/dM_H\rangle$, and $\langle\sigma^2(\nu_f;M)\rangle$. The resulting ("indirect") values are given in Table I, together with estimated standard deviations which are due both to the uncertainties of the mass widths and to the uncertainties of the assumptions made.

The assumptions of linearity of $\nu_L(M_L)$ and $\nu_H(M_H)$ with fragment mass [Eqs. (18) and (19)] are not the source of any significant error, because the equations developed on this basis are quite accurate first-order approximations. It may also be shown that the possible errors due to the other assumptions made [Eqs. (29) and (30)] are quite small. Although the correlation of ν_L and ν_H for a fixed mass ratio has been assumed to be zero [Eq. (30)] in the absence of information, there are limits in any case on the value of the conditional covariance. A general theorem about covariances[34] puts upper and lower bounds on this quantity:

$$-1\leqq C(\nu_L,\nu_H;M_H)/\sigma(\nu_L;M_L)\sigma(\nu_H;M_H)\leqq 1. \quad (36)$$

This corresponds to the statement that the conditional correlation coefficient of ν_L and ν_H is bounded by ±1. For positive correlation (i.e., large ν_L occurring with most probability for large ν_H) this strongly limits the covariance: $C(\nu_L,\nu_H;M_H)\leqq\frac{1}{4}\sigma^2(\nu)\cong0.3$. For negative correlation, there are other restrictions on the possible covariance, such as the physical limitation of ν_L and ν_H to small positive integers.

Consideration of the possible errors in the physical assumptions made above leads to estimated standard deviations of ±0.005 for $\langle d\nu/dM_H\rangle$, and ±0.007 for $\langle d\nu_L/dM_L\rangle$ and $\langle d\nu_H/dM_H\rangle$, from these sources of error. These uncertainties are negligible compared to the effect of present experimental uncertainties in the mass distributions, as seen in Table I.

All of the slopes $\langle d\nu_L/dM_L\rangle$ and $\langle d\nu_H/dM_H\rangle$ given in Table I are similar, averaging about 0.08 for light fragments and 0.10 for heavy fragments, as determined solely from mass data. These slopes are in reasonable agreement with the directly-measured data discussed in Sec. II. Equations (16), (17), and (22) allow weighted average values of $\langle d\nu_L/dM_L\rangle$, $\langle d\nu_H/dM_H\rangle$, and $\langle d\nu/dM_H\rangle$ to be calculated very simply from the published data on neutron yields. It is merely necessary to calculate covariances, such as $[\langle M_L\nu_L\rangle-\bar{M}_L\bar{\nu}_L]$, from the uncorrected mass yields, and divide by the corrected variance $\sigma^2(M_L)=\sigma^2(M_H)$.

This procedure automatically corrects for dispersion shift of neutron data points, and is an improvement over visual fitting or the unnecessary assumption of Gaussian distributions. The covariances $C(\nu_L,M_L)$ and $C(\nu_H,M_H)$ have the valuable property of invariance to symmetrical dispersion of mass, so that uncorrected mass data should yield the correct value. Unfortunately the calculated neutron efficiencies are definitely affected by dispersion shifts, and in any case are not too well known (see Appendix II). This limits the accuracy of slopes determined directly from experimental data. However, the slopes $\langle d\nu/dM_H\rangle$ determined directly in those experiments[7,13] in which angular correlation is not involved are not much affected by this drawback.

The published neutron yield data discussed earlier in this paper have been treated in this way to yield least square linear regression slopes, and the results are given at the bottom of Table I ("direct" values). There are no such data for $Pu^{239}+n$, and the data for $U^{233}+n$ and $U^{235}+n$ are in need of better neutron efficiency correction, which would probably increase all of their slopes. Hence the estimated standard deviations should be considered somewhat unsymmetrical. In view of this, the average directly-measured slopes $\langle d\nu_L/dM_L\rangle$ and $\langle d\nu_H/dM_H\rangle$ would probably be about 0.06 and 0.08, if accurate correction could be made.

As stated above, these values are in reasonable agreement with values given by mass-yield data. Because of the present lack of exact knowledge as to neutron-fragment correlation (see Appendix II), the neutron

[39] R. B. Leachman, Phys. Rev. **101**, 1005 (1956).

data determined from mass yields are often more trustworthy; their accuracy may be greatly improved by future improvements in mass-yield data.

IV. NEUTRON YIELDS FROM CUMULATIVE MASS DISTRIBUTIONS

Having found some simple relations between neutron emission and mass distributions by the powerful techniques of moments, averages, and correlations, we now proceed to extract the more detailed information on neutron emission which is still concealed in the mass distributions.[39a] It should be particularly noted that no result in this section, or in any other part of the paper, is based on the unnecessary assumption that any distribution is Gaussian (normal).

The method which will be used to determine $\nu_f(M)$ is essentially that of matching the initial and final cumulative yields of fission fragments. What is meant here by cumulative yield is the sum of the yields of all fragments of mass less than a given value. The symbol $y(M)$ will be used to mean the initial yield (before neutron emission) of mass number M, and $Y(M)$ will be the final yield, after neutron emission. Thus the initial and final cumulative yields for mass M_0 are, respectively, $\sum_0^{M_0} y(M)$ and $\sum_0^{M_0} Y(M)$.

The mass yields will be considered to be normalized in the usual way, to a total of 200% for binary fission. If essentially no symmetric fissions occur, each mass peak may be separately normalized to 100% total, which permits more accurate determination of final (radiochemical) cumulative mass yields and of $\nu_f(M)$. This is, in fact, possible for all four experimental cases to be considered here.

Neutron emission from fission fragments (assumed here to be the only source of neutrons) shifts the initial fragment masses to lower final masses. The exact relation between the two cumulative yields is given by

$$\begin{aligned}\sum_0^{M_0} Y(M)=&\sum_0^{M_0} y(M)+y(M_0+1)\\&\times[P_1(M_0+1)+P_2(M_0+1)+\cdots]\\&+y(M_0+2)[P_2(M_0+2)\\&\qquad+P_3(M_0+2)+\cdots]+\cdots,\end{aligned}\tag{37}$$

in which $P_\nu(M)$ is the probability that exactly ν neutrons will be emitted by an initial fission fragment of mass M. Since all quantities in Eq. (37) are non-negative, the final cumulative yield for a given mass M_0 is always greater than (or, conceivably, equal to) the initial cumulative yield:

$$\sum_0^{M_0} Y(M)\geqq\sum_0^{M_0} y(M).\tag{38}$$

This relation gives a useful check on the accuracy of cumulative yield data; if at any mass the final cumulative mass yield is less than the initial cumulative yield, then at least one of the two cumulative yields is wrong. It is apparent from Eq. (37) and from the identity

$$\nu_f(M)\equiv\sum_0^{\infty}\nu P_\nu(M)\tag{39}$$

that, for approximately constant mass yield values $y(M)$ and neutron emission probabilities $P_\nu(M)$, the two cumulative yields will differ by approximately $y(M)\nu_f(M)$. To obtain a more general relation between the cumulative yields from Eq. (37), we may treat $y(M)$, $P_\nu(M)$, and similar quantities, as continuous functions of mass, and expand them as Taylor series:

$$\begin{aligned}\sum_0^{M_0} Y(M)=&\sum_0^{M_0} y(M)+[y(M_0)+(dy/dM)+\cdots]\\&\times[P_1(M_0)+P_2(M_0)+\cdots\\&+(dP_1/dM)+(dP_2/dM)+\cdots]\\&+[y(M_0)+2(dy/dM)+\cdots]\\&\times[P_2(M_0)+P_3(M_0)+\cdots+2(dP_2/dM)\\&\qquad+2(dP_3/dM)+\cdots]+\cdots.\end{aligned}\tag{40}$$

This is equivalent to

$$\begin{aligned}\sum_0^{M_0} Y(M)=&\sum_0^{M_0} y(M)+y(M_0)\{\nu_f(M_0)+\tfrac{1}{2}(d/dM)\\&\times[\nu_f(M_0)+\langle\nu_f^2;M_0\rangle]\}+\tfrac{1}{2}(dy/dM)\\&\qquad\times[\nu_f(M_0)+\langle\nu_f^2;M_0\rangle]+\cdots.\end{aligned}\tag{41}$$

If the assumption is made that the conditional variance $\sigma^2(\nu_f;M)$ is a constant, this equation may be simplified:

$$\begin{aligned}\sum_0^{M_0} Y(M)=&\sum_0^{M_0} y(M)+\nu_f^*(M_0)y(M_0)\\&+\tfrac{1}{2}(dy/dM)[\nu_f(M_0)+\nu_f^2(M_0)\\&\qquad+\langle\sigma^2(\nu_f;M)\rangle]+\cdots.\end{aligned}\tag{42}$$

In this equation $\nu_f^*(M_0)\equiv\nu_f(M_0+\nu_f+\tfrac{1}{2})$, so that ν_f is to be evaluated at an initial mass value $\nu_f+\tfrac{1}{2}$ mass units higher than M_0. Consideration of higher-order terms shows that dy/dM is to be evaluated at the same mass as ν_f^*.

Further simplification results from the relation

$$\nu_f(M_0)+\nu_f^2(M_0)=2\sum_0^{\nu_f(M_0)} n,\tag{43}$$

which holds for integral values of $\nu_f(M_0)$, and from treating the cumulative distributions also as continuous

[39a] *Note added in proof.* H. Farrar and R. H. Tomlinson have used similar methods to obtain $\nu_f(M)$ (to be published).

functions of M:

$$\sum_{0}^{M0} Y(M) = \sum_{0}^{M_0+\nu_f^*(M_0)} y(M) + \tfrac{1}{2}(dy/dM)\langle\sigma^2(\nu_f; M)\rangle + \cdots. \quad (44)$$

The values of $\nu_f(M)$ of physical interest are those at integral values of the mass number M, so that Eq. (44) is more useful when rewritten as the final result,

$$\sum_{0}^{M_0-\nu_f(M_0)-\frac{1}{2}} Y(M) = \sum_{0}^{M_0-\frac{1}{2}} y(M) + \tfrac{1}{2}(dy/dM)\langle\sigma^2(\nu_f; M)\rangle + \cdots, \quad (45)$$

in which both $\nu_f(M_0)$ and dy/dM are to be evaluated at M_0.

Higher-order correction terms have been evaluated, but will not be given here, because they may be shown to have small effect. Even the first-order correction term given in Eq. (45) has a relatively minor effect in determining $\nu_f(M)$, usually changing ν_f by considerably less than 0.1.

Although it is necessary to treat cumulative mass distributions and other quantities as continuous functions of mass in order to derive and use Eq. (45), this really causes no difficulty in practice. It is a simple matter to interpolate smoothly between discrete values of the cumulative final mass distribution, and the initial mass distribution is automatically obtained as a continuous distribution because of experimental mass dispersion. Thus what is really meant by $\sum_0^{M_0-\frac{1}{2}} y(M)$ is $\int_0^{M_0} y(M)dM$, after correction for resolution.

It is only necessary to match the cumulative initial mass yield, corrected by $\frac{1}{2}(dy/dM)\langle\sigma^2(\nu_f;M)\rangle$, to the interpolated final cumulative mass yield to obtain $\nu_f(M)$ for all values of the initial mass M. This method should work, in principle, even at symmetric fission, though uncertainties in the cumulative yields make this presently a hypothetical remark. Equation (45) may be used even for three-humped fission, discussed in Sec. V. In any case the calculated $\nu_f(M)$ includes delayed neutrons, and is probably slightly smoothed.

That this method of determining $\nu_f(M)$ is highly accurate, given accurate mass data, has been established by many numerical examples. It has been found that the error introduced by Eq. (45) is ordinarily about 0.01 in $\nu_f(M)$, although the error may be nearer 0.05 if the trend of $\nu_f(M)$ changes sharply. Such errors are not significant in the present state of knowledge of neutron and mass yields. Error could also be introduced if $\langle\sigma^2(\nu_f;M)\rangle$ were greatly different from the values given in Table I. This could only occur if very high correlation of light- and heavy-fragment excitations does in fact exist, contrary to the assumption of Eq. (30). The standard deviations for $\langle\sigma^2(\nu_f;M)\rangle$ quoted in Table I allow for lack of knowledge on the correlation, and make the correction term in Eq. (45) uncertain by about 50%.

The major source of error in determining $\nu_f(M)$ from Eq. (45), however, lies in the mass yield data, both initial (radiochemical and mass-spectrometric) and final (time-of-flight). Typical cumulative yield data—though more accurate than usual—are shown in Fig. 5 for thermal neutron fission of U^{235}. The final mass yields, taken from Walker's compilation,[28] are so complete in this case that very little interpolation is necessary. If either of Katcoff's compilations[24,25] had been used, instead, the differences (amounting to the order of 0.01 for ν_f, for instance) would be invisible in Fig. 5. The initial mass yields are based on the average of Stein's data[21] with that of Milton and Fraser,[22] corrected for mass resolution[12] (see Appendix III). This correction to the cumulative yield is small except at the extreme ends of the mass distribution for either peak, near symmetry and extreme asymmetry—and it is not a large correction there.

Because the mass yields near symmetrical fission are so small for $U^{235}+n$ fission, it is possible to normalize the total yield in each peak to 100%. The cumulative initial yields shown in Fig. 5 have been plotted as $\sum_0^{M_L} y(M)$ for the light peak and $\sum_{A-M_L}^{A} y(M)$ for the heavy peak, so as to allow a single set of points to represent both light and heavy initial fragment yields. The final yields are plotted in a similar way. The final cumulative yield of light fragments is displaced horizontally (along the mass axis) from the initial cumulative yield by approximately $\nu_L(M)$ at each point, and similarly with the heavy fragments.

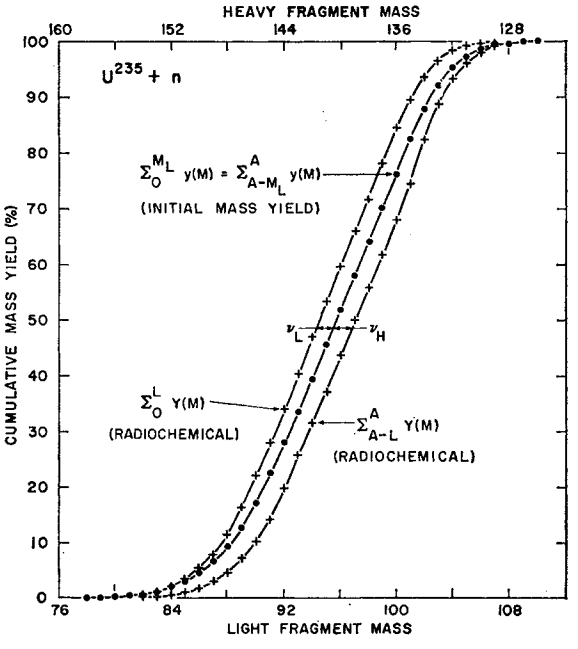

FIG. 5. Cumulative mass yields used in determining neutron yields, for fission of $U^{235}+n$. The horizontal distances between cumulative yield curves, with slight corrections for curvature, determine neutron yields ν_L and ν_H as functions of initial fragment mass.

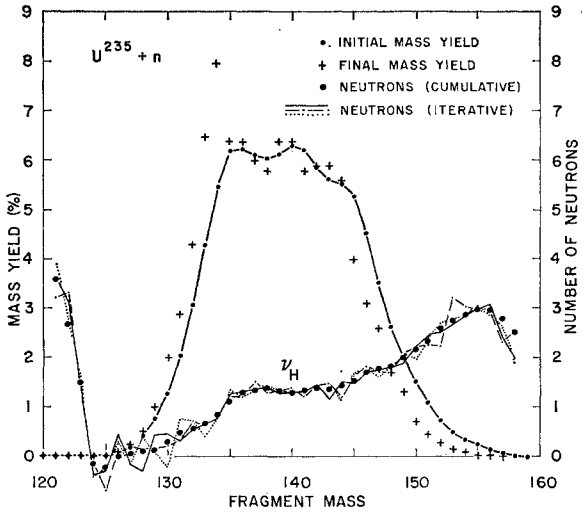

FIG. 6. Neutron yields for heavy fragments in fission of $U^{235}+n$, determined from cumulative mass yields, and shown as a function of initial fragment mass in this and the following figures. The initial and final mass yields used (some interpolated) are shown. Also shown are several possible alternative solutions for the neutron yields, determined by iterative means. The best average of these iterative solutions appears to be the result obtained from cumulative mass yields.

Thus the mass displacement between light and heavy cumulative yields in this graph is a measure of $\nu(M_H)=\nu_L(A-M_H)+\nu_H(M_H)$ for each mass ratio. Since the initial cumulative yield points must always lie between the two final yield points for the same mass ratio [Eq. (38)], it would be possible to obtain $\nu(M_H)$ with fair accuracy from the final mass data alone. This may be necessary if radiochemical yields should be determined in the absence of corresponding time-of-flight data.

The cumulative yields shown in Fig. 5 are obviously consistent—that is, they do not cross each other—over a wide range of mass. The crossing of initial and final cumulative yields actually occurs here in the vicinity of masses 84 and 127, corresponding to cumulative yields of 2% and 99.8% in Fig. 5. In both cases the inconsistency could be eliminated by different interpolation of missing final yields.

Figure 6 shows the same mass yields as in Fig. 5 in noncumulative form, for the heavy peak only. This peak is of special interest because of the unusually high final yield of mass 134, which has been interpreted[40–46] as evidence for fine structure in the primary fission process.

Also shown are the fragment neutron yields $\nu_H(M_H)$ which may be deduced from the cumulative mass yields, using Eq. (45). Although a complete set of these neutron yields is given in Fig. 5 (heavy points), not all of these points are equally reliable. In particular, the neutron yields at the extreme edges of the peak are less reliable because of uncertainties in the cumulative yields. Obviously the negative values of $\nu_H(M_H)$ in the vicinity of mass 125 are not to be taken serously, although the true neutron yield is doubtless very small here.

It is of considerable interest to know whether the values of $\nu_H(M_H)$ deduced from cumulative mass yields can actually produce a sharp peak in the final mass yields from a relatively smooth initial mass distribution. Because of the importance of this question, it was investigated in several different ways.

First, hypothetical values of $P_\nu(M)$ were assigned to every heavy fragment mass number in such a way as to exactly reproduce $\nu_H(M_H)$ as calculated from Eq. (45), and to have the proper conditional variance, $\sigma^2(\nu_H;M_H)\cong 0.61$ (see Table I). Using these assumed neutron emission probabilities, the final yields $Y(M)$ were then calculated from the initial yields $y(M)$ shown in Fig. 6, using Eq. (37). The results were very similar to the desired final yields shown in Fig. 6, and the peak at mass 134, in particular, was very well reproduced. This was true of each of several such assumed sets of $P_\nu(M)$.

Secondly, and more elaborately, a number of sets of $P_\nu(M)$ were worked out which would lead *exactly* from the given initial mass yields to the given final mass yields, with no assumptions as to required values of $\nu_H(M_H)$. The method used was an iterative process, in which values of $P_\nu(M)$ were arbitrarily chosen, one by one, beginning at either end of the fragment mass distribution. Negative values of P_ν were not allowed, nor were overly-large positive values, since $\sum_0^\infty P_\nu$ for a given mass must equal 1.0. Negative values of ν were not used, except where necessary in the vicinity of mass 125. This process was carried out a number of times, in various ways, and the resulting values of $\nu_H(M_H)$ calculated. Three typical sets of values of $\nu_H(M_H)$ produced by this arbitrary iterative process, with $\sigma^2(\nu_H;M_H)\cong 0.61$, are shown in Fig. 6. There are fluctuations in $\nu_H(M_H)$ from set to set—in fact, the iterative process is somewhat unstable, in that the mass-to-mass fluctuations tend to grow as the mathematical process is carried out. However, all of the iterative solutions follow very closely the trend of $\nu_H(M_H)$ as determined from cumulative mass distributions. It seems very likely that the average of a large number of the possible iterative solutions would be almost precisely the smooth cumulative solution. Thus the cumulative solution is presumably the best solution to the problem.

Finally, an attempt was made to find an arbitrary hypothetical set of $P_\nu(M)$ which would combine the virtues of the sets discussed above, yielding precisely the given values of $\nu_H(M_H)$ and at the same time leading

[40] D. R. Wiles, B. W. Smith, R. Horsley, and H. G. Thode, Can. J. Phys. **31**, 419 (1953).
[41] D. R. Wiles and C. D. Coryell, Phys. Rev. **96**, 696 (1954).
[42] L. E. Glendenin, E. P. Steinberg, M. G. Inghram, and D. C. Hess, Phys. Rev. **84**, 860 (1951).
[43] E. P. Steinberg, L. E. Glendenin, M. G. Inghram, and R. J. Hayden, Phys. Rev. **95**, 867 (1954).
[44] E. P. Steinberg and L. E. Glendenin, *Proceedings of the International Conference on the Peaceful Uses of Atomic Energy, Geneva 1955* (United Nations, New York, 1956), Vol. 7, p. 3.
[45] A. C. Pappas, Laboratory for Nuclear Science, Massachusetts Institute of Technology, Report No. 63, 1953 (unpublished).
[46] R. B. Leachman and H. W. Schmitt, Phys. Rev. **96**, 1366 (1954).

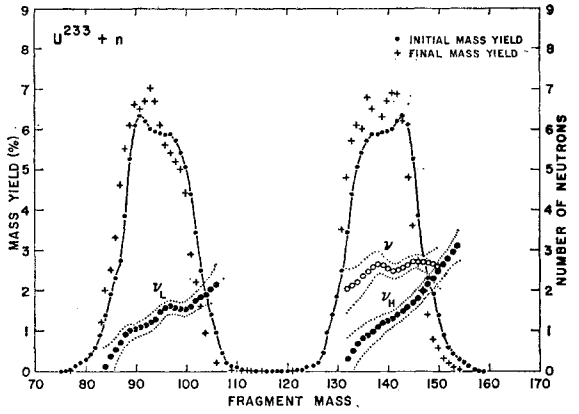

FIG. 7. Neutron yields for fission of $U^{233}+n$, derived from cumulative mass yields, and shown as a function of initial fragment mass. Also shown are the measured initial and final mass yields used. Estimated standard deviations are shown by dotted lines in this and the following three figures.

from the initial yields $y(M)$ to the exact values of $Y(M)$ desired. In order to make the results most significant physically, the same restrictions were imposed—that all emission probabilities be positive or zero, and refer to non-negative numbers of neutrons, and that the emission probabilities form a smoothly varying set, with $\sigma^2(\nu_H;M_H)\cong 0.61$. Such a set was found, without great difficulty (but not given here), which would yield precisely the necessary experimental values of $Y(M)$ from the highest mass value (mass 158) down to mass 126. At this point the required value of ν_H is negative, because of the slight inconsistency between experimental initial and final yields. Since the negative values of ν_H would be of no physical significance in any case, the somewhat tedious process of determining a suitable set of $P_\nu(M)$ was not carried out all the way to symmetric fission (mass 118). That the process is mathematically possible is indicated by the precise agreement between $\bar{\nu}_H$ as calculated from the cumulative solution for $\nu_H(M_H)$ and from $\bar{M}_H-\bar{H}$ [Eq. (3)]; the value in both cases is 1.310.

Thus it is clear that the values $\nu_H(M_H)$ determined by matching cumulative mass distributions can, with reasonable distributions of neutron emission probabilities, lead *precisely* from the experimentally determined initial mass yields to the experimentally determined final mass yields. The occasional sharp peaks in final mass yield, and numerous smaller irregularities, can all be readily explained in terms of slight changes in neutron emission probabilities from mass to mass. A sharp peak in the final mass yield at mass 134 is easily produced by a change in slope of the ν_H values seen at about mass 136. A similar explanation accounts for the smaller final yield peak at mass 100 for $U^{235}+n$ (see Fig. 8). Sudden dips in the final yields can be produced by very slight irregularities in $\nu_f(M)$.

Thus the final (radiochemical) mass yields are extremely sensitive to slight changes in $\nu_f(M)$, or $P_\nu(M)$. Conversely, the values of $\nu_f(M)$ determined from cumulative mass yields are rather insensitive to sizable fluctuations in the mass yields. This is fortunate, from the standpoint of determining the values of $\nu_f(M)$. It should not be inferred that this investigation has ruled out fine structure in the initial fission process as a possible cause of fine structure in the final mass yields. There is evidence of some fine structure in the initial yields, as may be seen in Figs. 6–10. What has been established is merely that such an explanation—involving so far unseen sharp peaks in initial fragment mass yields—is not necessary. Slight neutron emission variations can produce such peaks with ease.

The method of determining $\nu_f(M)$ given by Eq. (45) has been applied to four experimental sets of fission mass yields; the results are seen in Figs. 7 to 10. The sets of fission data are the same ones discussed in the previous section, for thermal neutron fission of U^{233}, U^{235}, and Pu^{239}, and for spontaneous fission of Cf^{252}. The initial mass distributions are in each case averages of time-of-flight data of Milton and Fraser[9,22] and of Stein and Whetstone,[8,21] corrected for experimental resolution as described in the previous section. The final mass distributions are from radiochemical and mass-spectrometric data as compiled by Walker,[28] except for Cf^{252} yields, which are mostly based on Nervik's compilation,[29] with some additions[30,31] and some interpolations. All of the measured mass yields used, both initial and final, are shown in Figs. 7 to 10. Interpolated final yields are not shown; it is obvious from the figures that there are gaps in the measured final yield data which need to be filled.

The values of $\nu_f(M)$ determined from these mass yields are shown in Figs. 7 to 10 wherever they are considered to be of meaningful accuracy. No ν_f values are shown in regions of sparse or nonexistent final mass yields, or of very doubtful initial mass yields; it is hoped that future mass data will allow extension of these results. The value of the total neutron number, $\nu=\nu_L+\nu_H$, is also shown as a function of the heavy fragment mass.

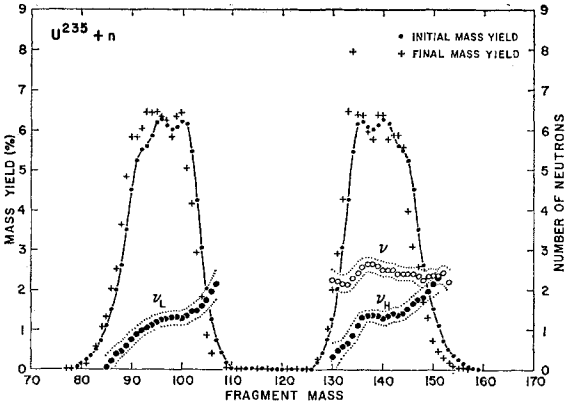

FIG. 8. Neutron yields for fission of $U^{235}+n$, derived from cumulative mass yields. Also shown are the measured mass yields used.

It could equally well, of course, have been shown as a function of light-fragment mass, or of the mass ratio.

Estimated standard deviations are indicated in Figs. 7 to 10 by light dotted lines above and below the ν_f points. It would be somewhat misleading to attach individual error bars to each point, as the possible errors are by no means independent for each point. In estimating these uncertainties, allowance has been made for uncertainty in the initial and final mass yield data and errors in the resolution correction of initial mass yields. Possible additional errors due to the method are so trivial compared to those due to the mass data that they do not appreciably increase the uncertainty.

The uncertainty in each cumulative mass yield was estimated at each mass number. An arbitrary minimum error in the cumulative yield, amounting to 10% of the individual (noncumulative) mass yield at each point, was adopted. This corresponds to an error of ± 0.1 in ν_f due to the initial cumulative yield, and an equal error due to the final yield, or an overall minimum error of ± 0.14 in ν_f. This minimum error corresponds to that produced by about 6% standard deviation for each individual mass yield, if due to random causes. The uncertainty was taken to be larger in cases of interpolated final mass yields, conflicting data, or statistically uncertain yields. The large uncertainties in ν_f data for Cf^{252} (Fig. 10) are due largely to the discrepancies between the time-of-flight data from Los Alamos[8] and that from Chalk River.[9] These standard deviations for Cf^{252} may be too conservative, as they include the entire effect of adopting either one of these conflicting sets of data instead of using the average.[23a]

The uncertainties in $\nu = \nu_L + \nu_H$ are estimated on the same basis. These results depend mostly on the cumulative final yields, and are almost immune to errors in the initial (time-of-flight) mass yields. Thus the data on ν may on occasion be more accurate than that for either ν_L or ν_H, as is the case for Cf^{252} in Fig. 10.

As has been pointed out earlier in this section, the results for ν_f are not sensitive to small peaks and valleys

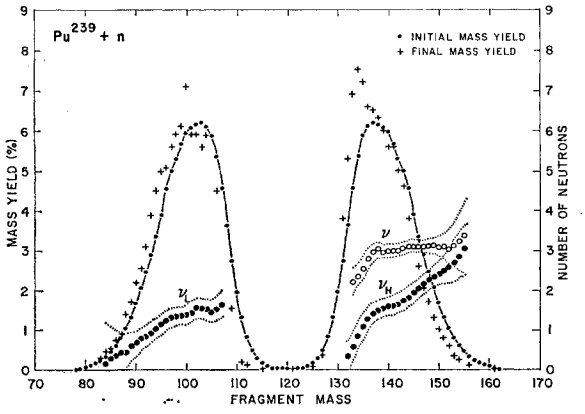

FIG. 9. Neutron yields for fission of $Pu^{239}+n$, derived from cumulative mass yields. Also shown are the measured mass yields used.

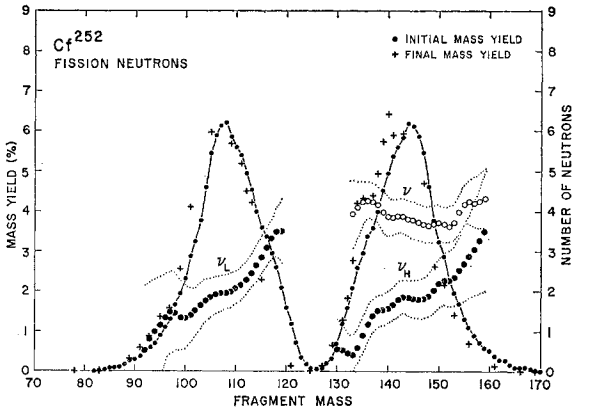

FIG. 10. Neutron yields for fission of Cf^{252}, derived from cumulative mass yields. Also shown are the measured mass yields used.

in the mass yields, as the sensitivity is in the other direction. Similarly, the smoothing of time-of-flight data which is desirable in removing large mass dispersions,[12] or in the case of large statistical uncertainties, has an almost negligible effect on the calculated neutron yields (ordinarily changing them by less than 0.05), as was verified in several cases.

The ν_f results were also found to be virtually unchanged when an entirely different method of removing dispersion was used. This method, which was used several years ago[47] in calculating ν_f for $U^{233}+n$ and $U^{235}+n$, was that of fitting the time-of-flight data with the sum of two Gaussian distributions in each peak. This is a total of four Gaussian distributions, but the symmetry of the initial mass distribution about the mass $A/2$ means that only two Gaussians are independent. The fitting was done by means of the central moments of the distribution, up through $\mu_5(M)$. The effects of experimental mass dispersion could be removed easily either by applying Sheppard's corrections[10] to the moments or by suitably decreasing the width of each Gaussian distribution.

Such a bimodal distribution gives a very smooth representation of the initial mass yield data, corrected for dispersion. A trimodal representation would allow central moments up through μ_8 to be fitted, but would probably require computing machine calculations. These methods were not used in the results reported in this paper, because of the discovery of simpler and more general methods[12] of removing dispersion. Although the bimodal fitting did not reproduce the apparent fine structure in the initial mass yields, the calculated neutron yields $\nu_f(M)$ were virtually unaffected by this omission.

V. DISCUSSION

It is apparent from Figs. 7 to 10 that the average number of neutrons emitted from individual fragments,

[47] J. Terrell, in Atomic Energy Commission Reports WASH-1021, 1959, and WASH-1026, 1959 (unpublished).

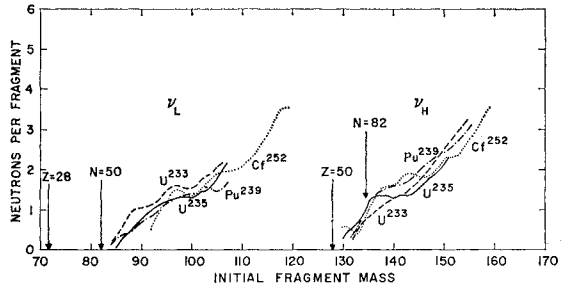

FIG. 11. Summary of neutron yields derived from cumulative mass yields, as functions of initial fragment mass. The approximate initial fragment masses corresponding to various magic numbers are shown (based on constant charge-to-mass ratio for initial fragments).

$\nu_f(M)$, varies considerably with mass, and furthermore is not precisely linear with mass even within a single mass peak. The variations of $\nu_f(M)$, and of $\nu(M_H)$, are similar to those of neutron numbers determined directly, as seen in Figs. 1 to 4. The similarities are considerably increased by applying, where possible, necessary corrections to the direct data on $\nu_f(M)$ for dispersion shift and angular correlation. Although this can be done only incompletely and with some uncertainty, the substantial agreement between the directly and indirectly measured neutron data gives more weight to both sets of data.

The average slopes $\langle d\nu_L/dM_L\rangle$ and $\langle d\nu_H/dM_H\rangle$ could be determined from the data points given in Figs. 7 to 10, but may be more precisely determined from the same mass data by the use of moments as in Sec. III-C. These slopes average around 0.08 and 0.10 neutrons per unit mass change in the light and heavy peaks, respectively, as given in Table I. Also given in Table I are the slopes estimated from direct neutron counting, which, after correction, might average about 0.06 and 0.08, as discussed in Sec. III-C.

The similarity of the results for neutron emission from four different fissioning nuclides may be seen more strikingly by plotting all of the data in a single graph, as has been done in Fig. 11. Evidently the neutron yield as a function of mass could be represented rather accurately by a single curve, at least for these four cases. The yield of neutrons is seen to drop nearly to zero at about masses 82 and 128 in each case. These masses are of particular interest in that both correspond very nearly to the magnic number 50, for neutrons and protons, respectively. The magic-number locations shown in Fig. 11 were calculated on the assumption that the initial fragments have the same ratio of charge to mass as the parent fissioning nuclide (constant charge ratio); the locations differ only trivially for these four cases.

Figure 11 is almost identical with an earlier graph, shown at an American Physical Society meeting,[48] in which the results for U^{233}, U^{235}, and Pu^{239} were based on the time-of-flight data of Stein[21] alone. Since that time it has been possible to incorporate the data of Milton and Fraser,[22] but the results are little changed, in general.

Because of the similarity of the various sets of data shown in Fig. 11, all may be represented fairly well by a single curve for $\nu_f(M)$. Such a curve would rise roughly linearly with mass above $M=82$, and above $M=128$. In the central mass range $118\leqq M\leqq 128$ the value of $\nu_f(M)$ would presumably decrease smoothly with mass in such a way as to connect the two measured parts of the curve. Such a representation has already been used by Milton and Fraser.[49]

It is probably more than a coincidence that the points of near-zero neutron yield, as seen in Fig. 11, correspond to the magic numbers $N=50$ and $Z=50$. Possibly also the magic number $N=82$ has some connection with a change in slope of $\nu_f(M)$ near mass 136. The magic number $Z=28$ would occur near mass 72, which is perhaps too low in mass to have much influence on the fission process.

If the data on $\nu_f(M)$ are represented approximately by two straight lines in the light and heavy fragment regions, the value of ν for asymmetric fission should be given by their sum,

$$\nu\cong 0.08(M_L-82)+0.10(M_H-126). \tag{46}$$

The mass number 126 is used here instead of 128 because it gives a better linear representation. The average total neutron yield $\bar{\nu}$ should thus be given, for asymmetric fission, by

$$\bar{\nu}\cong 0.08(A-204.5)+0.02(\bar{M}_H-140). \tag{47}$$

The particular representation in terms of $(\bar{M}_H-140)$ was chosen for convenience merely because $\bar{M}_H$ is often nearly equal to 140. However, $\bar{M}_H$ for asymmetric fission is less than 140 for a lighter fissioning nuclide[50] such as $Ra^{226}+p$.

Equation (47), for neutron fission of U^{233}, U^{235}, and Pu^{239}, and for spontaneous fission of Cf^{252}, gives $\bar{\nu}$ values of 2.35, 2.52, 2.83, and 3.88, respectively.[50a] These numbers differ by about 0.1 from the best measured values (see Table I). Thus it seems likely that a part of the general tendency for $\bar{\nu}$ to increase with A may be explained in terms of the increase of ν_L and ν_H with fragment mass. Obviously this concept should not be pushed too far, since $\bar{\nu}$ is also known to increase with increasing excitation energy of the fissioning nuclide, at the rate of perhaps 0.14 neutrons per MeV. However, part of this increase of $\bar{\nu}$ with excitation may be due to changes in the fission product distribution.

Asymmetric fission seems to be characterized[51] by $N_L>50$, $Z_H>50$, or approximately, $M_L>82$, $M_H>128$.

[48] J. Terrell, Bull. Am. Phys. Soc. **6**, 16 (1961).

[49] J. C. D. Milton and J. S. Fraser, Phys. Rev. Letters **7**, 67 (1961).

[50] R. C. Jensen and A. W. Fairhall, Phys. Rev. **109**, 942 (1958).

[50a] *Note added in proof.* The "universal curve" of Figs. 12 and 13 gives 2.42, 2.58, 2.83, and 3.83 for these cases.

[51] H. W. Newson, Phys. Rev. **122**, 1224 (1961).

These limits seem to define quite accurately the regions of appreciable mass yield for asymmetric fission. They also seem to be the points at which neutron yield nearly vanishes. It is likely that there is a nonrandom relation between these two factors, such that the near-zero neutron yield of magic-number fragments is connected with the near-vanishing fragment yields at these same masses.

It is interesting to note that the width of asymmetric fission peaks seems to narrow with decreasing A, until in the vicinity of mass 210 asymmetric fission no longer seems to occur, as pointed out by Newson.[51] The latter case is exemplified by Fairhall's work[52] on fission of $Bi^{209}+D$, in which only a single symmetric mass peak is found. A similar result has been found by Duffield, Schmitt, and Sharp,[19] for photofission of Bi^{209}. Fairhall's data are shown in Fig. 12, along with his estimated smooth final yield curve. It is apparent that the symmetric fission mass yields here are limited, perhaps coincidentally, by $N_L>50$ and $Z_H<50$. Also shown are the hypothetical neutron yields which would be predicted by the "universal neutron yield curve" derived from Fig. 11. The neutron yield from both fragments would be predicted to vanish at the same mass ratio for which mass yields vanish, since for $A\cong 208$ the magic numbers $N_L=50$ and $Z_H=50$ occur for a single mass ratio. Fairhall estimated $\bar{\nu}$ to be about 4 from the final mass yields. This would also be the prediction of the $\nu_f(M)$ curve shown, which would also predict essentially zero values of ν for asymmetric fission. The limits $N_L>50$ and $Z_H>50$ would allow asymmetric fission here only in the narrow range of mass numbers 126 to 128.

These same speculative concepts may be applied with considerable success to the case of three-humped fission mass yields, exemplified by the data of Jensen and Fairhall[50] for $Ra^{226}+p$. These mass yields are shown in Fig. 13, with the smooth yield curve estimated by

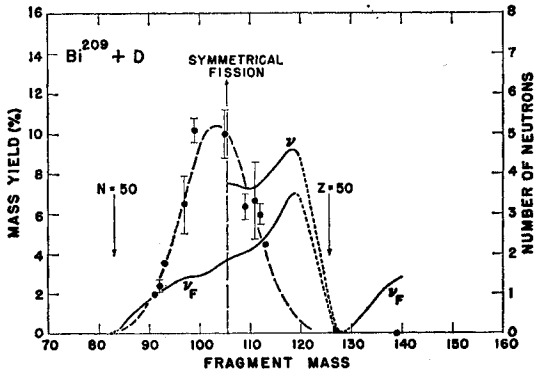

FIG. 12. Radiochemical (final) mass yields for fission of $Bi^{209}+D$ (data of Fairhall), together with hypothetical neutron yields based on the idea of a universal function $\nu_f(M)$. Approximate initial fragment masses corresponding to $N=50$ and $Z=50$ are shown.

[52] A. W. Fairhall, Phys. Rev. **102**, 1335 (1956).

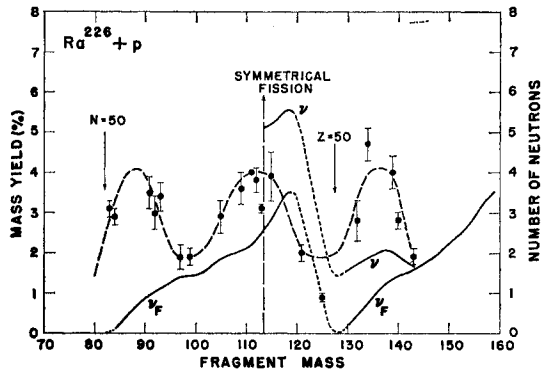

FIG. 13. Radiochemical (final) mass yields for fission of $Ra^{226}+p$ (data of Jensen and Fairhall), together with hypothetical neutron yields based on the idea of a universal function $\nu_f(M)$. Approximate initial fragment masses corresponding to $N=50$ and $Z=50$ are shown.

Jensen and Fairhall and with the hypothetical neutron yields predicted on the basis of Fig. 11. Once again asymmetric fission seems to be bounded by $N=50$ and $Z=50$, and symmetric fission by $Z=50$, at which point the mass yield is quite low. The hypothetical neutron yield curve would predict a high value of ν for symmetric fission and a low value for asymmetric fission, with an average $\bar{\nu}$ of 3 or 4. Jensen and Fairhall estimate $\bar{\nu}$ to be in the range 3 to 5, which is in good agreement. If more radiochemical yields were known for this case, the actual variation of $\nu(M_H)$ could be determined, by the methods described in this paper. When the method of cumulative yields was tentatively applied to the radiochemical data of Jensen and Fairhall, with many missing yields being filled in by interpolation, it was found that, indeed, the ν value is higher for symmetric fission than for the asymmetric peak, and is lowest for $Z=50$. The yield data are too incomplete, however, to make this result trustworthy, as different interpolation could no doubt yield a different result.

Other cases of three-humped fission have been found in this mass region by Fairhall *et al.*,[53,54] Nobles and Leachman,[55] Duffield *et al.*,[19] and Britt *et al.*[56] In those cases where mass yields have been accurately determined the magic numbers $N=50$ and $Z=50$ (masses 82 and 128, approximately) correspond to low mass yields. Mass 82 seems to correspond to a near-absolute cutoff for fission yields. However, Sugihara *et al.*[57] found about 0.3% of fissions for $Bi^{209}+p$ yielding light-fragment masses less than about 78.

[53] A. W. Fairhall, R. C. Jensen, and E. F. Neuzil, *Proceedings of the Second United Nations International Conference on the Peaceful Uses of Atomic Energy, Geneva, 1958* (United Nations, Geneva, 1958), Vol. 15, p. 452.

[54] R. C. Jensen and A. W. Fairhall, Phys. Rev. **118**, 771 (1960).

[55] R. A. Nobles and R. B. Leachman, Nuclear Phys. **5**, 211 (1958).

[56] H. C. Britt, H. E. Wegner, and J. Gursky, Phys. Rev. Letters **8**, 98 (1962).

[57] T. T. Sugihara, J. Roesmer, and J. W. Meadows, Jr., Phys. Rev. **121**, 1179 (1961).

The hypothetical neutron yields discussed above cannot at present be checked against other experimental data than that from which they were derived. The concept of a universal function $\nu_f(M)$ is obviously of only limited validity, and most details of the curve used in Figs. 12 and 13 should not be given much weight. However, the concept may be a useful guide in predicting fission data not yet measured. Milton and Fraser[49] have had some success in correlating fission fragment kinetic energies with total energy release in this way, for the same four cases shown in Fig. 11. The hypothetical neutron yield curve would predict greatly increased values of $\bar{\nu}$ for near-symmetrical neutron-induced fission of U^{233}, U^{235}, and Pu^{239}. This may be connected with the decreased fragment kinetic energies in this region, as pointed out by Milton and Fraser.[49] Because of its greater mass number A, symmetrical fission for Cf^{252} would, in contrast, correspond to *low* neutron yield (both fragments near the magic number $Z=50$), which may be correlated with the apparent maximum in kinetic energy for Cf^{252} in this region.[49]

If the minimum neutron yield at about mass 128 and the maximum near 119 are actually correctly located, the neutron yield effects discussed earlier in this paper should lead to a local minimum in final mass yield at about mass 125, and a local maximum near mass 113. These general effects would, of course, be in addition to various other maxima and minima due to minor fluctuations in $\nu_f(M)$, perhaps different for each fissioning nuclide. A combination of the smoothed hypothetical neutron yield curve of Figs. 12 and 13 with a uniform initial mass yield curve gives the minimum at mass 125 and a maximum at mass 112 and 113, in addition to a general lowering of final mass yield in the region 116–126.

The evidence against which these predictions may be checked is not very extensive. However, Walker[28] finds the mass-125 final yield to be unusually low in three cases of neutron-induced fission (U^{233}, U^{235}, and Pu^{239}). Jensen and Fairhall[50] also found a low yield for mass 125 in fission of $Ra^{226}+p$. The data for low yield at mass 125 are not overpowering in any of these cases. As to the possible high final yield near mass 113, the rapidly varying mass yields in this region for U^{233}, U^{235}, and Cf^{252}, and missing yield data for Pu^{239}, make the prediction difficult to check. It is interesting, though, that Colby, Shoaf, and Cobble[58] found unusually high yields for final masses 113 and 115 in the fission of $U^{233}+He^4$. In this case it seems possible that one of the three humps in the final mass yield is due purely to neutron emission effects, and that the initial mass yield may have only two peaks. No third peak was in fact visible in the time-of-flight data of Whetstone and Leachman.[59]

It is interesting to speculate on the physical reasons for the unusual behavior of $\nu_f(M)$, as seen in Fig. 11 and throughout this paper. The "neck" model of Whetstone[6] and the similar ideas of Vladimirskii[60] do not appear to be quite adequate to account for the full behavior of $\nu_f(M)$, in particular the vanishingly low neutron yields at $N=50$ and $Z=50$. The apparent importance of $Z=50$ is emphasized by the tendency of heavy-fragment charge not to drop below this figure, as pointed out recently by Wahl *et al.*[61] and by Milton.[22]

Why should magic numbers, and particularly the magic number 50, be so important in the fission process? Nuclei with magic numbers have a well-known tendency to be spherical in shape,[62] and hence have smaller maximum radii than nonmagic nuclei. This property would lead to higher Coulomb energies for fission fragments on the point of scission, if one is magic. If both fragments were nonmagic and elongated, it is obvious that they could be brought into contact with less expenditure of Coulomb energy than if one of the fragments were spherical, and possibly of unusually small radius. Thus the magic pairs of fragments would have a higher fission barrier to overcome, and would presumably be produced in lower yield. They might also have a higher final kinetic energy upon completion of the fission process. There is evidence that this is so[49] for $Z=50$, which is about where the kinetic energy of fragments is maximum. It is difficult to say if there is any extra kinetic energy for $N=50$, as the available data[49] either just barely touch this region, or do not reach it at all, as in the case of Cf^{252}.

Whether the total fragment excitation (and total ν) would be larger or smaller in these magic cases would depend on the balance between total Coulomb energy and total mass release, both of which would presumably be increased in these cases.

It is obvious that one or both of the fission fragments must be considerably distorted by excitation at scission, as the total kinetic energy of the fragments is, for most types of fission, about equal to the Coulomb energy of two spherical fragments in contact,[4] with radii $1.82\,M^{\frac{1}{3}}$ (giving $E_K \cong 0.121\,Z^2/A^{\frac{1}{3}}$). This radius is at least 25% larger than normal radii, and indicates considerable fragment distortion. If this large effective radius of scission were due purely to ellipsoidal deformation, the assumptions of collinearity and unchanged density (corresponding to $r_0=1.4\times10^{-13}$ cm) would lead to a ratio of about 1.6 between major and minor axes of each fragment.[63] The center-to-center separation would be about 7% more than for the case of tangent spheres. However, it is possible that the excited fragments may have less-than-normal density. In any case, there is not enough energy released in low-energy fission to permit

[58] L. J. Colby, Jr., M. L. Shoaf, and J. W. Cobble, Phys. Rev. **121**, 1415 (1961).

[59] S. L. Whetstone, Jr., and R. B. Leachman, Bull. Am. Phys. Soc. **6**, 376 (1961).

[60] V. V. Vladimirskii, Zhur. Eksp. i Teoret. Fiz. **32**, 822 (1957) [translation: Soviet Phys.—JETP **5**, 673 (1957)].

[61] A. C. Wahl, R. L. Ferguson, D. R. Nethaway, D. E. Troutner, and K. Wolfsberg, Phys. Rev. **126**, 1112 (1962).

[62] L. Wilets, Science **129**, 361 (1959).

[63] Based on ellipsoidal calculations of S. Cohen and W. J. Swiatecki, Aarhus University Report, 1961 (unpublished).

two undistorted fragments to be in contact. Thus the Coulomb fission barrier must have a very strong influence on selection of permissible types of fission fragments and excitations.

In this situation, why does the magic fragment get none, or almost none, of the excitation energy? The explanation may be the already-invoked spherical preferences of magic nuclei. These nuclei are believed, on considerable evidence, to have great resistance to deformation from a near-spherical shape, or in effect a high surface tension.[64] Thus the more-easily distorted nonmagic nucleus should be more readily increased in maximum radius by excitation than the spherical magic nucleus. The fission barrier, then, could be more easily lowered by excitation of the nonmagic nucleus.

This explanation in terms of deformability and maximum radius of excited fragments may well be the reason, then, why the magic numbers $N=50$ and $Z=50$ correspond to very low neutron emission. Other properties of $Z=50$, such as the greater mass-release in fission when one fragment is magic, may account for the apparent preference of the charge[22,61] for $Z=50$. Why $N=82$ is apparently less important in fission is not known. Perhaps it is less magic in its effect on nuclear radii.

These considerations as to nuclear radius should presumably be of less importance for fission induced by very high-energy particles, when the process takes place well above the fission barrier and probably with extreme rapidity. At higher inducing energies it is, indeed, observed that fission mass distributions are broader and that the low yield at $Z=50$ is less prominent.[53,54] The demarkation point between symmetric and asymmetric fission thus tends to vanish at these higher excitations, but $N=50$ still appears to be the effective lower limit of the fission mass distribution.

ACKNOWLEDGMENTS

The author would like to thank S. L. Whetstone, J. C. D. Milton, J. S. Fraser, and H. R. Bowman and his co-workers for the use of some of their data before publication. Discussions with B. C. Diven, J. J. Griffin, J. R. Huizenga, R. B. Leachman, J. H. Manley, J. C. D. Milton, and S. L. Whetstone have helped in clarifying some of the ideas presented here. The author is particularly indebted to G. P. Ford of this Laboratory for calling attention to the virtues of distribution moments and correlation coefficients.

APPENDIX I. FISSION NEUTRON EMISSION ENERGIES

A factor of major importance in fission research is the emission energy spectrum of the emitted neutrons. Knowledge of this spectrum is vital to estimation of neutron-fragment correlation (Appendix II), as in the direct measurements of $\nu_f(M)$ described in this paper, and to correction of initial fragment mass data for neutron emission effects (Appendix III). Unfortunately, the neutron emission spectrum is very difficult to measure directly.

However, considerable information on the center-of-mass emission spectrum may be obtained from the more accessible laboratory spectrum of fission neutrons. This information was to some extent developed in an earlier paper,[4] but the present analysis goes further. It is, like the earlier analysis, based on the assumptions that the neutrons are emitted from the fragments, and that the fragments have their maximum velocity at the time. These assumptions are in good agreement with the evidence for low energy fission; at high energies it seems clear that some neutrons are emitted before fission. Even if some fraction of the neutrons in low-energy fission are emitted from the fissioning nuclide and not from the fragments, the results given here should be approximately correct if the fraction is small. The evidence is that the fraction of neutrons not emitted by the fragments is indeed small,[65] or zero.

For a neutron emitted by a fragment, the laboratory energy E, center-of-mass energy $E_{\text{c.m.}}$ of the neutron, fragment energy per nucleon E_f, and center-of-mass angle of emission $\theta_{\text{c.m.}}$ are related by

$$E=E_f+E_{\text{c.m.}}+2(E_fE_{\text{c.m.}})^{\frac{1}{2}}\cos\theta_{\text{c.m.}}. \qquad \text{(A1)}$$

The energy E_f is more accurately defined as the neutron energy corresponding to the initial velocity of the fragment, i.e., of the fragment center-of-mass system. The emission angle $\theta_{\text{c.m.}}$ and center-of-mass energy $E_{\text{c.m.}}$ are both to be measured with respect to this initial motion of the fragment; the fragment motion is, of course, altered by recoil in the emission process.

The further assumption of symmetry of emission of neutrons in the forward and backward directions, or, less restrictively,

$$\langle\cos\theta_{\text{c.m.}}\rangle=0, \qquad \text{(A2)}$$

leads to a simple relation between the average energies,

$$\bar{E}=\bar{E}_f+\bar{E}_{\text{c.m.}}. \qquad \text{(A3)}$$

In all of these equations an average is denoted either by a bar or by angular brackets. It should be understood here that these averages are weighted by neutron emission.

Equations (A1) and (A2), with the slight additional assumption that $\theta_{\text{c.m.}}$ is independent of E_f and $E_{\text{c.m.}}$, also lead to a relation between variances:

$$\sigma^2(E)=\sigma^2(E_f)+\sigma^2(E_{\text{c.m.}}) +4\langle E_fE_{\text{c.m.}}\rangle\langle\cos^2\theta_{\text{c.m.}}\rangle+2C(E_f,E_{\text{c.m.}}). \qquad \text{(A4)}$$

[64] J. P. Elliott and A. M. Lane, in *Encyclopedia of Physics*, edited by S. Flügge (Springer-Verlag, Berlin, 1957), Vol. 39, pp. 241–410, especially p. 315; S. Moszkowski, *ibid.*, pp. 411–550, especially pp. 497–516; D. L. Hill, *ibid.*, pp. 178–240, especially pp. 237–238.

[65] H. R. Bowman, S. G. Thompson, J. C. D. Milton, and W. J. Swiatecki, Phys. Rev. (to be published).

TABLE II. Fission neutron energy data. The symbols E, $E_{c.m.}$, and E_f represent neutron energy in the laboratory system, neutron energy in the fragment center-of-mass system, and neutron energy corresponding to fragment velocity. The neutron-weighted values of E_f for light and heavy fragment groups are denoted by $\bar{E}_{lf}$ and $\bar{E}_{hf}$; the averages not weighted by neutron emission probability are $\langle E_L m/M_L\rangle$ and $\langle E_H m/M_H\rangle$. The symbol E_K denotes total initial fragment energy. The symbols σ^2 and C refer to variance and covariance. Averages are indicated by bars or angular brackets. Estimated standard deviations are given for all quantities.

	$U^{233}+n$	$U^{235}+n$	$Pu^{239}+n$	Cf^{252}
$\bar{E}$[a] (MeV)	1.98 ±0.05	1.95 ±0.05	2.03 ±0.05	2.15 ±0.08
$\bar{E}_K$[a] MeV)	165±2	167±2	173±2	183±3
$\langle E_L m/M_L\rangle$[b] (MeV)	1.055±0.015	1.043±0.015	1.015±0.014	0.977±0.018
$\langle E_H m/M_H\rangle$[b] (MeV)	0.485±0.007	0.493±0.007	0.527±0.007	0.557±0.010
$\bar{E}_{lf}$[c] (MeV)	1.02 ±0.02	1.01 ±0.02	0.98 ±0.02	0.94 ±0.02
$\bar{E}_{hf}$[c] (MeV)	0.46 ±0.01	0.48 ±0.01	0.50 ±0.01	0.54 ±0.01
$\bar{E}_f$[d] (MeV)	0.74 ±0.02	0.74 ±0.02	0.74 ±0.02	0.74 ±0.02
$\bar{E}_{c.m.}$[e] (MeV)	1.24 ±0.05	1.21 ±0.05	1.29 ±0.05	1.41 ±0.08
$\sigma^2(E)$[f]	2.61 ±0.13	2.53 ±0.13	2.74 ±0.14	3.08 ±0.23
$\sigma^2(E_f)$[g]	0.082±0.004	0.074±0.004	0.062±0.003	0.045±0.003
$2C(E_f,E_{c.m.})$[g]	0±0.02	0±0.02	0±0.02	0±0.02
$4\langle E_f E_{c.m.}\rangle\langle\cos^2\theta_{c.m.}\rangle$[g]	1.22 ±0.08	1.19 ±0.08	1.27 ±0.08	1.39 ±0.11
$\sigma^2(E_{c.m.})$[h]	1.31 ±0.10	1.27 ±0.10	1.41 ±0.11	1.65 ±0.17
$\sigma^2(E_{c.m.})/\bar{E}_{c.m.}^2$	0.85 ±0.05	0.87 ±0.05	0.85 ±0.05	0.83 ±0.04

[a] Based on various experiments; see text and reference 4.
[b] Average values not weighted by neutron emission; corrected for neutron mass $m=1.009$.
[c] Average values weighted by neutron emission, and corrected for neutron mass 1.009.
[d] Average of $\bar{E}_{lf}$ and $\bar{E}_{hf}$, based on $\bar{\nu}_L/\bar{\nu}_H=1.0\pm0.1$.
[e] From Eq. (A3).
[f] Based on a Maxwellian distribution of E, and on Eq. (A6). Possible errors due to this assumption are not included in this table.
[g] Based on isotropic emission ($b=0\pm0.2$).
[h] From Eq. (A4).

The quantities $\sigma^2(E)$, $\sigma^2(E_f)$, and $\sigma^2(E_{c.m.})$, are the variances or second central moments of the various energies; an example is $\sigma^2(E)\equiv\langle E^2\rangle-\bar{E}^2$. The quantity C is the covariance; by definition, as throughout this paper, $C(E_f,E_{c.m.})\equiv\langle E_f E_{c.m.}\rangle-\bar{E}_f\bar{E}_{c.m.}$.

Equations (A3) and (A4) make it possible to determine both the average energy $\bar{E}_{c.m.}$ and the variance $\sigma^2(E_{c.m.})$ of the emission spectrum from existing data, primarily on the laboratory fission spectrum and on fragment velocities. The rest of this section will be devoted mainly to this process of evaluation.

A number of measurements on the laboratory fission neutron spectrum have been published recently. Some of these are "age" measurements[66–68] and have, fortunately, removed the long-standing discrepancy[69] between these measurements and other data on the fission neutron spectrum. The other recent experiments[65,70–73] are more direct measurements of the fission neutron spectrum, and are generally in excellent agreement with previous data. Two previously unmeasured spectra have been reported.[70,74] The data[74] for thermal neutron fission of Pu^{241} give a Maxwellian shape, an average energy of 2.002±0.051 MeV, and $\bar{\nu}=2.88\pm0.18$. The average energy and neutron number are in good agreement with a theoretical relationship[4] between these quantities [Eq. (A9), below]. On the other hand, the average energy[70] for spontanteous fission of Pu^{240}, 1.78±06 MeV, is unusually low, and not in good agreement with the predicted value 1.91 MeV.

On the basis of these more recent experiments in combination with the older data, the best average laboratory energies ($\bar{E}$) are essentially the same as estimated earlier,[4] and are given in Table II. Also on the basis of these experiments, the laboratory energy spectrum is accurately described by a Maxwellian distribution,

$$N(E)=(2/\pi^{\frac{1}{2}}T^{\frac{3}{2}})E^{\frac{1}{2}}e^{-E/T}, \qquad \text{(A5)}$$

in which T is a parameter describing the average laboratory energy, $\bar{E}=3T/2$. This simple distribution is, fortunately, also the prediction of evaporation theory.[4]

A Maxwellian distribution in energy has a simple variance,[75]

$$\sigma^2(E)=\tfrac{2}{3}\bar{E}^2. \qquad \text{(A6)}$$

The variances $\sigma^2(E)$ which are tabulated in Table II are calculated on this basis. Since the laboratory spectrum is sometimes described as a Watt spectrum,[4,76] it is of interest to know how accurately Eq. (A6) describes the actual variance. The Watt spectrum is given by

$$N(E)=\text{const}\times e^{-E/T}\sinh[2(EE_f)^{\frac{1}{2}}/T], \qquad \text{(A7)}$$

[66] D. B. Lombard and C. H. Blanchard, Nuclear Sci. and Eng. **7**, 448 (1960).
[67] R. C. Doerner, R. J. Armani, W. E. Zagotta, and F. H. Martens, Nuclear Sci. and Eng. **9**, 221 (1961).
[68] W. G. Pettus, Nuclear Sci. and Eng. **8**, 171 (1960).
[69] H. Goldstein, P. F. Zweifel, and D. G. Foster, Jr., *Proceedings of the Second United Nations International Conference on the Peaceful Uses of Atomic Energy, Geneva, 1958* (United Nations, Geneva, 1958), Vol. 16, p. 379.
[70] T. W. Bonner, Nuclear Phys. **23**, 116 (1961).
[71] J. Grundl and A. Usner, Nuclear Sci. and Eng. **8**, 598 (1961).
[72] A. B. Smith, P. R. Fields, R. K. Sjoblom, and J. H. Roberts, Phys. Rev. **114**, 1351 (1959).
[73] L. Stewart, Nuclear Sci. and Eng. **8**, 595 (1960).
[74] A. B. Smith, R. K. Sjoblom, and J. H. Roberts, Phys. Rev. **123**, 2140 (1961).
[75] An energy spectrum of the form $E^n e^{-E/T}$ has average energy $\bar{E}=(n+1)T$, and variance $\sigma^2(E)=(n+1)T^2=\bar{E}^2/(n+1)$.
[76] B. E. Watt, Phys. Rev. **87**, 1037 (1952).

and has average energy $\bar{E}=E_f+3T/2$. Its variance may be shown to be $\sigma^2(E)=\frac{2}{3}(\bar{E}^2-E_f^2)$, so that it is a slightly more narrow energy distribution than the Maxwellian, for a given average energy. The parameter E_f should not be considered to be the actual fragment energy per nucleon, as the values of E_f which have been quoted as fitting the spectrum are always less[4] than the true value of $\bar{E}_f$. A typical quoted value[76] of the parameter E_f is 0.5 MeV. This would give a variance lower by 0.167 than a Maxwellian distribution, or about a 6% decrease in σ^2.

In order to investigate the variance of the laboratory spectrum more directly, the average energy and variance were calculated for the $U^{235}+n$ photoplate data of Frye and Rosen,[77] which represent the most complete single set of data published (0.35 to 12 MeV). It was, of course, necessary to extrapolate the data beyond the limits of measurement, and this was done on the basis of the Maxwellian distribution fitted to the data by the authors. The result of the calculation was $\bar{E}=1.959$ MeV, $\sigma^2(E)=2.489=0.648\,\bar{E}^2$, after correcting for grouping of data.[10] This result is thus very close to the variance of a Maxwellian distribution, amounting to 97.3% of the predicted value $\frac{2}{3}\bar{E}^2$ (the rms variation σ is 98.6% of that for a Maxwellian). Thus the use of the Maxwellian result, Eq. (A6), seems reasonably well justified in calculating $\sigma^2(E)$. Possible errors due to the use of this equation have not been included in Table II, as the dependence of both $\bar{E}$ and $\sigma^2(E)$ on the distribution assumed in fitting data complicates the estimation of such errors.

The average fragment energy per nucleon, $\bar{E}_f$, was estimated as 0.78 ± 0.02 MeV in the earlier paper.[4] It now appears that 0.74 ± 0.02 MeV is a better figure. This result is based on fragment kinetic energy data[4,22] essentially the same as used before, but is lowered on the basis of two considerations.

First, it now appears likely that $\bar{\nu}_L\cong\bar{\nu}_H$, so that average values of $\bar{E}_f$ for the light and heavy fragments should be given roughly equal weighting (see Appendix II). The second new consideration which results in a lower value for $\bar{E}_f$ is the effect of variation of ν_f with M. It is now well-established that more neutrons are emitted by the heavier light fragments, and by the heavier heavy fragments. In both cases, neutron emission weights the value of $\bar{E}_f$ on the side of lower velocities. Consideration of this factor leads to the neutron-weighted average value of the neutron energy E_Lm/M_L corresponding to fragment velocity, denoted by $\bar{E}_{lf}$,

$$\bar{E}_{lf}\equiv\left\langle\frac{\nu_L m E_L}{\bar{\nu}_L M_L}\right\rangle=\frac{\bar{E}_K m\bar{M}_H}{A\bar{M}_L}\left[1+\frac{A\sigma^2(M_L)}{\bar{M}_H\bar{M}_L{}^2}-\frac{AC(E_K,M_L)}{\bar{E}_K\bar{M}_H\bar{M}_L}-\frac{A\sigma^2(M_L)}{\bar{M}_H\bar{M}_L\bar{\nu}_L}\cdot\left\langle\frac{d\nu_L}{dM_L}\right\rangle+\cdots\right],\quad\text{(A8)}$$

in which E_K is the initial total kinetic energy of the two fragments, before neutron emission, and E_L is the kinetic energy of the light fragment. The symbol m represents the mass of the neutron, 1.009; the difference between fragment mass and mass number M is so small that it is neglected in this appendix. The other symbols have the usual meaning as given elsewhere in this paper, and averages here are weighted only by numbers of fissions unless otherwise specified. The value of $\bar{E}_{hf}$, the neutron-weighted average value of E_Hm/M_H, is given by an expression similar to Eq. (A8), with subscripts interchanged (E_H is the initial kinetic energy of the heavy fragment).

The first two correction terms in the brackets of Eq. (A8) are small, as pointed out elsewhere,[4] amounting in sum to 0.0025 ± 0.0005 for light fragments and 0.008 ± 0.001 for heavy fragments, for any of the four cases considered here. However, the last correction term is quite appreciable, reducing $\bar{E}_f$ by 3 or 4% for the values of $\langle d\nu_L/dM_L\rangle$ and $\langle d\nu_H/dM_H\rangle$ derived in this paper (Table I, indirect values). The correlation of ν_f and M is thus more important than was believed earlier,[4] the difference being due to the larger values of the slopes which are derived in this paper.

The specially weighted average values of $\bar{E}_{lf}$ and $\bar{E}_{hf}$ are given in Table II, together with the values of $\bar{E}_K$, $\langle E_Lm/M_L\rangle$, and $\langle E_Hm/M_H\rangle$ (not weighted by neutron emission) from which they are derived. The average of $\bar{E}_{lf}$ and $\bar{E}_{hf}$ is $\bar{E}_f=0.74\pm0.02$ MeV in each case, based on $\bar{\nu}_L/\bar{\nu}_H=1.0\pm0.1$.[78] With this slightly lower value of $\bar{E}_f$, evaporation theory considerations[4] now lead to the numerical relation

$$\bar{E}\cong0.74+0.653(\bar{\nu}+1)^{\frac{1}{2}}(\text{MeV}).\quad\text{(A9)}$$

The second term represents $\bar{E}_{\text{c.m.}}$; the constant has been chosen to fit the $U^{235}+n$ data, but the other three points fit exceedingly well. This re-evaluation of the constant corresponds, as before, to average fragment nuclear temperatures of 0.6 to 0.7 MeV, but the nuclear temperature constant[79] a is 11 MeV^{-1} instead of the value 12 ± 2 found earlier[4] for fission fragments.

The variance $\sigma^2(E_f)$, which is also necessary in using Eq. (A4), is primarily due to the difference between $\bar{E}_{lf}$ and $\bar{E}_{hf}$. The calculated variances $\sigma^2(E_f)$ given in Table II also include a total contribution of about 0.004 due to the spread of velocities within each of the two mass peaks. The covariance $C(E_f,E_{\text{c.m.}})$ which appears in Eq. (A4) has not been determined experimentally, but may be estimated to be small. The only direct evidence on this matter is the recent data of Bowman *et al.*[65] for Cf^{252}, in which the spectrum of $E_{\text{c.m.}}$ was found to be essentially the same for both light and heavy fragments. On the basis of evaporation theory

[77] L. Cranberg, G. Frye, N. Nereson, and L. Rosen, Phys. Rev. **103**, 662 (1956).

[78] If the alternative assumption $\bar{\nu}_L=1.1\bar{\nu}_H$ were made, the value of $\bar{E}_f$ would be 0.75 MeV, 0.01 MeV higher.

[79] The nuclear temperature constant a is defined by $a=E_x/T^2$, in which E_x is the nuclear excitation energy and T is the nuclear temperature.

it would be expected that higher fragment excitations (and larger ν_f) would be associated with higher temperatures (and larger $E_{c.m.}$). Thus the value of $\bar{E}_{c.m.}$ might be expected to increase through each mass peak, as $\nu_f(M)$ increases with mass. However, the same considerations might lead to the expectation of a lower average $\bar{E}_{c.m.}$ for the heavy mass peak, if the nuclear temperature coefficient[79] a is proportional to fragment mass number in this mass region. Both effects would lead to small covariances of the same order (0.01), but of opposite sign. Hence $C(E_f,E_{c.m.})$ has been taken as 0.00 ± 0.01 in Table II.

With this value of covariance, the average value $\langle E_f E_{c.m.}\rangle$, also appearing in Eq. (A4), is equal to the product of averages, $\bar{E}_f\bar{E}_{c.m.}$. The other factor in this term, $\langle\cos^2\theta_{c.m.}\rangle$, is equal to $\frac{1}{3}$ if neutrons are emitted isotropically. If emission is not isotropic and is described by a factor $(1+b\cos^2\theta_{c.m.})$, then[80] $\langle\cos^2\theta_{c.m.}\rangle=(1+3b/5)/(3+b)$. However, the evidence[65] suggests nearly isotropic emission. The values of $4\langle E_f E_{c.m.}\rangle\langle\cos^2\theta_{c.m.}\rangle$ appearing in Table II are based on isotropy, with $b=0\pm0.2$.

Thus all of the terms in Eq. (A4) except $\sigma^2(E_{c.m.})$ are known, or can be estimated with reasonable accuracy, and the resulting values of $\sigma^2(E_{c.m.})$ are given in Table II. On the basis of the available data, then, it may be seen that

$$\sigma^2(E_{c.m.})\cong0.85\bar{E}_{c.m.}^2. \tag{A10}$$

The emission spectrum thus must be considerably broader than a Maxwellian distribution. For any of these four cases, this variance $\sigma^2(E_{c.m.})$ would be accurately obtained by representing the center-of-mass spectrum as the sum of two normalized Maxwellian distributions,[81] differing in average energy by $\Delta\bar{E}_{c.m.}=0.85$ MeV.[82] This is similar to the result of evaporation theory calculations,[4] which gave $\Delta\bar{E}_{c.m.}\cong0.6$ MeV.

The most direct experimental determination of the emission spectrum, that of Bowman *et al.*[65] on Cf^{252}, gave results for $_{c.m.}$ and $\sigma^2(E_{c.m.})$, as determined by three-temperature fits (1.44 ± 0.08 MeV and 1.64MeV^2), which are remarkably close to those in Table II (1.41 ± 0.08 MeV and 1.65 MeV^2). However, there is always a possibility of systematic error with a highly energy-sensitive neutron detector. In addition, only the data from one laboratory angle (11.25° with respect to either fragment direction) covers the range below $E_{c.m.}=0.1$ MeV, and evaporation spectrum calculations[4] are also in some doubt below 0.1 MeV. Unfortunately, it is this emission energy range which is most responsible for angular correlation of neutrons and fragments, as has been pointed out before,[4] and is discussed further in Appendix II. Nevertheless, there is excellent agreement between experimental[65] and theoretical[4] emission spectra for Cf^{252}. This seems also to be the case in 14-MeV neutron fission[83] of U^{235}.

Thus the same conclusion follows from direct experiment, indirect data, and theory—the neutron emission spectrum is broader than a single Maxwellian distribution [Eq. (A5)]. This seems to be a clear result in spite of some uncertainties in the experimental data. If the assumption of isotropic emission were dropped, for instance, an anisotropy factor $b\cong1.3$ would be required for consistency of Eq. (A4) with a Maxwellian emission spectrum. This appears to be well outside of the amount of anisotropy consistent with experiment.[65] Thus the emission spectrum of fission neutrons should be represented by the sum of two Maxwellian distributions, or by some equally broad spectrum, in fission calculations. The basic reason for the large variance is, according to evaporation theory, the wide range of fission fragment temperatures.[4]

However, it should be kept in mind that the emission spectrum width calculated in this section from Eq. (A4) is that of the over-all spectrum, the sum of spectra from both fragments. It is possible, though unlikely,[65] that the emission spectra from light and heavy fragments are quite different, and in this case each might be somewhat narrower than indicated here. Another possibility is that the correlation of excitations in the two fragments is not zero, in contradiction to the assumption of Eq. (30). This would have some effect on evaporation theory calculations,[4] and conceivably—for positive correlation of excitations—could lead to a narrower emission spectrum. However, the agreement between theory and experiment, as to the emission spectrum, is reasonably good for the assumption $C(\nu_L,\nu_H;M_H)=0$.

APPENDIX II. FISSION NEUTRON ANGULAR CORRELATION, AND ν_L/ν_H

Direct measurements of neutron numbers as functions of fragment mass, $\nu_f(M)$, depend critically on the directional correlation of fission fragments and fission neutrons. Correction for varying neutron counter efficiency due to varying correlation is the major correction to the neutron data, and may be seriously in error if the wrong emission spectrum (see Appendix I) is assumed. In the present section some new angular distribution relations are given, the corrections applied in other papers are discussed, and the result $\bar{\nu}_L\cong\bar{\nu}_H$ is derived.

It is assumed here, as elsewhere, that the neutrons are emitted from fragments which have their maximum velocities. The basic problem is a transformation from

[80] If anisotropy is, instead, described by $1+A_2[\frac{3}{2}\cos^2\theta_{c.m.}-\frac{1}{2}]$, then $\langle\cos^2\theta_{c.m.}\rangle=\frac{1}{3}(1+2A_2/5)$. The relation between A_2 and b is: $b=3A_2/(2-A_2)$.

[81] This variance would also be obtained for an emission spectrum of the form $E^{0.18}e^{-E/T}$ (see footnote 75).

[82] The added variance in energy due to using the sum of two normalized Maxwellian distributions, differing in average energy by $\Delta\bar{E}_{c.m.}$, is $(5/12)(\Delta\bar{E}_{c.m.})^2$.

[83] Yu. A. Vasilev, Yu. S. Zamyatnin, E. I. Sirotinin, and E. F. Fomushkin, Atomnaya Energ. **9**, 449 (1960) [translation: Soviet J. Atomic Energy **9**, 990 (1961)].

the energy and angular distributions in the center-of-mass system of a fragment to the corresponding laboratory distribution. Calculation of the Jacobian[84] gives the basic result,

$$N(E,\theta)=(E/E_{\text{c.m.}})^{\frac{1}{2}}N_{\text{c.m.}}(E_{\text{c.m.}},\theta_{\text{c.m.}}), \quad \text{(A11)}$$

in which N and $N_{\text{c.m.}}$ are the corresponding neutron yields in laboratory and center-of-mass systems, per unit energy range and solid angle. The energies and angles are defined in Appendix I, and are related by Eq. (A1).

If the emission spectrum were Maxwellian (Eq. A5) and isotropic, Eq. (A11) would become

$$N(E,\theta)=\tfrac{1}{2}(E/\pi^3T^3)^{\frac{1}{2}} \times\exp\{-[E+E_f-2(EE_f)^{\frac{1}{2}}\cos\theta]/T\}. \quad \text{(A12)}$$

Integration of this equation over the energy spectrum leads to the over-all laboratory angular distribution for this case,

$$N(\theta)=(1/4\pi)[1+(2E_f/T)\cos^2\theta] \times\{1+P[(2E_f/T)^{\frac{1}{2}}\cos\theta]\}\exp[-(E_f/T)\sin^2\theta] +(1/2\pi)(E_f/\pi T)^{\frac{1}{2}}\exp(-E_f/T). \quad \text{(A13)}$$

The symbol $P(x)$ refers to the normal probability integral,[85]

$$P(x)\equiv(2\pi)^{-\frac{1}{2}}\int_{-x}^{x}\exp(-t^2/2)dt. \quad \text{(A14)}$$

Equations (A12) and (A13) are essentially as given by Ramanna *et al.*,[86] except that here the normalization factor is furnished (for a total integral of unity).

In some of the more recent experiments[6,13] on $\nu_f(M)$ the neutrons were detected by flat-response liquid scintillation counters subtending a large solid angle. What is needed for efficiency correction in these cases is the integral of the angular distribution $N(\theta)$ from $\theta=0$ to some limiting angle θ_m. For isotropic Maxwellian emission this may be shown to be

$$I(\theta_m)\equiv\int_0^{\theta_m}N(\theta)2\pi\sin\theta d\theta =\tfrac{1}{2}+\tfrac{1}{2}P[(2E_f/T)^{\frac{1}{2}}] -\tfrac{1}{2}\exp[-(E_f/T)\sin^2\theta_m]\cos\theta_m \times\{1+P[(2E_f/T)^{\frac{1}{2}}\cos\theta_m]\}. \quad \text{(A15)}$$

Equations (A12), (A13), and (A15) have obvious extensions to the case of two fission fragment velocities, and to an emission spectrum equal to the sum of two Maxwellian distributions (Appendix I), both of which changes are necessary to agree more closely with the physical situation. These equations also have obvious applications in correcting for neutrons detected backward from fragments. More elaborate formulas would be necessary to deal with anisotropic emission.

The use of a double Maxwellian emission spectrum leads to higher correlation between neutron and fragment directions, because of the increased probability of small emission energies. This gives 8 or 10% more neutron yield at 0°, using Eq. (A13), for the double Maxwellian spectrum derived in Appendix I, as compared to a single Maxwellian distribution of the same average energy. This increase drops to 6% for a neutron counter subtending an angle extending to $\theta_m=30°$ (approximately as in the work of Apalin *et al.*[13]) using Eq. (A15). For $\theta_m=90°$, most of the emitted neutrons enter the counter, regardless of the spectrum assumed. The broader spectrum increases the calculated efficiency only by about 0.4% in this case (Whetstone's experimental arrangement[6,8]). Whetstone used a broad spectrum in his corrections.

Apalin *et al.*,[13] however, actually calculated their neutron efficiencies on the basis of the narrowest possible emission spectrum, a single energy $E_{\text{c.m.}}$ for any given fragment mass. This gives calculated efficiencies for $\theta=0$ about a factor of 2 less than a more realistic spectrum, and a ratio of efficiencies for neutrons emitted by light and heavy fragments about 17% less than for the spectrum derived in Appendix I. However, the inclusion of all neutrons up to $\theta=30°$, for this broad spectrum, would considerably reduce the difference, to about 8% as compared to the 0° single-energy correction. Even this last procedure would not be correct, as the collimated fission chamber used by Apalin *et al.* also permitted a considerable range of fragment angles.

The angular correlation correction made to the data points shown in Fig. 4 is only an approximate correction. However, it is more accurate than that originally made by Apalin *et al.*[13] Their assumption of fixed $E_{\text{c.m.}}$ for a given mass leads, for isotropic emission, to the laboratory angular distribution[4]

$$Y(\theta)=E/4\pi E_{\text{c.m.}}|\cos(\theta_{\text{c.m.}}-\theta)|. \quad \text{(A16)}$$

However, they calculated only the 0° yield, $E/4\pi E_{\text{c.m.}}$. For $E_{\text{c.m.}}$ they chose $\bar{E}_{\text{c.m.}}=0.84+0.25\nu_f$ (MeV), an average of the estimates of Terrell[4,87] and of Bondarenko *et al.*[88] This infinitely narrow emission spectrum does not lead to sufficient angular correlation, because of the lack of very low energy neutrons. There is also no indication in the paper of Apalin *et al.* as to whether the fragment velocities were calculated for constant total

[84] If the neutron yields are given per unit energy range and *angle* (not solid angle), the Jacobian is $J(E_{\text{c.m.}},\theta_{\text{c.m.}};E,\theta)=1$.

[85] *Tables of Normal Probability Functions*, National Bureau of Standards, Applied Mathematics Series No. 23 (U. S. Government Printing Office, Washington, D. C., 1953).

[86] R. Ramanna, R. Chaudhry, S. S. Kapoor, K. Mikke, S. R. S. Murthy, and P. N. Rama Rao, Nuclear Phys. **25**, 136 (1961).

[87] Evaporation theory alone [see Eq. (A9)] would give the relation $\bar{E}_{\text{c.m.}}\cong0.653(2\nu_f+1)^{\frac{1}{2}}\cong0.78+0.35\nu_f$ for $\bar{\nu}=2.42$.

[88] I. I. Bondarenko *et al.*, *Proceedings of the Second United Nations International Conference on the Peaceful Uses of Atomic Energy, Geneva, 1958* (United Nations, Geneva, 1958), Vol. 15, p. 353.

energy E_K, or for the considerable variation in E_K which is seen experimentally.[49] Whatever their assumption, the same one is inherent in the re-correction made here.

What was done in obtaining the corrected results shown in Fig. 4 was to remove the original efficiency correction from the data and to recorrect on the basis of a Maxwellian emission spectrum for $\theta=0°$ (for simplicity), using Eq. (A13). The re-correction used the shifted mass values of Fig. 4 and was normalized[32] to $\bar{\nu}=2.42$. The same relation between $\bar{E}_{\text{c.m.}}$ and ν_f as was used in the original paper was retained, for simplicity, and no correction was made for neutrons emitted and detected backward. A more exact correction would also involve averaging the neutron detection efficiency over the range of angle subtended by the neutron detector, as well as over the fragment directions permitted by the collimator. Apalin *et al.* did not do this, and since they did not give full information on their geometry, no attempt was made here to arrive at the best correction for neutron efficiency.

As was mentioned in Sec. II, the approximate re-correction makes a considerable difference in their results. The ratio $\bar{\nu}_L/\bar{\nu}_H$, reported by Apalin *et al.* as 1.17 (and given as 1.23 by their graphs), is reduced by recorrection to 1.04. This figure should not be taken too seriously, as it might be changed by a more precise correction.

Ramanna *et al.*[86] used Eqs. (A13) and (A14) in their paper on angular correlation and energies of fission neutrons. They found it necessary to assume $\bar{\nu}_L/\bar{\nu}_H=1.3$ to fit their angular distribution data. However, this result is due largely to their assumption of the value 1.47 MeV for $\bar{E}_{\text{c.m.}}$ of $U^{235}+n$ fission, 20% higher than the value indicated by experiment (1.21 MeV in Table II). It is also due in part to their use of a single Maxwellian emission spectrum. The use of $\bar{E}_{\text{c.m.}}=1.21$ MeV and a double Maxwellian emission spectrum leads to a calculated angular distribution in excellent agreement with their results, for $\bar{\nu}_L/\bar{\nu}_H=1.0$. The agreement is perhaps even better than Ramanna *et al.* obtained, with quite different assumptions.

Some earlier angular correlation experiments, discussed in reference 4, also gave a result similar to that reported by Ramanna *et al.*, and others,[89] $\bar{\nu}_L/\bar{\nu}_H\cong 1.3$. However, such ratios seem in every case to be the result of unrealistic assumptions about the neutron emission spectrum, as in the two cases discussed above. Recently Bowman *et al.*[65] have obtained $\bar{\nu}_L/\bar{\nu}_H=1.16\pm0.01$ from least-square processing of their Cf^{252} data. However, Whetstone has obtained 1.02 ± 0.02 for this ratio in Cf^{252}, using an emission spectrum[4] based on evaporation theory, different fragment velocities, and a flat-response liquid scintillator.

Thus, from the discussion in this section, it seems clear that angular correlation calculations are highly sensitive to the emission spectrum assumed, and to other factors, and that $\bar{\nu}_L/\bar{\nu}_H=1.0\pm0.1$ is perhaps the most reasonable interpretation of the various experimental results. This ratio does not have much effect on the emission spectrum properties deduced in Appendix I, so that the argument is not circular. However, angular correlation corrections must still be considered somewhat tentative, in the absence of full information on neutron emission.

APPENDIX III. EFFECT OF NEUTRON EMISSION ON FRAGMENT VELOCITIES AND ENERGIES, AND ON APPARENT MASS RATIOS

The mass resolution of recent time-of-flight fission-fragment data is largely determined by neutron emission effects. To an even larger extent this is true of recent mass data obtained from the ratio of fragment energies, as determined by solid-state counter measurements.[56,90] The relations necessary to correct such initial-mass data for neutron effects are developed here.

A. Fragment Velocity Data

Fission fragment velocities are essentially unchanged, on the average, by neutron emission, as Stein was the first to point out.[21] Adding to the initial fragment velocity v_f the recoil velocity $mv_{\text{c.m.}}/M^*$, due to the emission of a neutron of mass m and center-of-mass velocity $v_{\text{c.m.}}$ at angle $\theta_{\text{c.m.}}$, by a fragment of resulting mass M^*, gives

$$v_f^{*2}=v_f^2+(mv_{\text{c.m.}}/M^*)^2-(2mv_{\text{c.m.}}v_f/M^*)\cos\theta_{\text{c.m.}}. \quad \text{(A17)}$$

Here v_f^* is the resulting velocity of the fragment, after emission of one neutron.

The assumptions of isotropic emission and of no correlation between $v_{\text{c.m.}}$ and $\theta_{\text{c.m.}}$ lead to simple averages for v_f^* and v_f^{*2}, for given M^* and v_f:

$$\langle v_f^*\rangle=v_f[1+\tfrac{1}{3}(m/M^*v_f)^2\langle v_{\text{c.m.}}^2\rangle-\cdots], \quad \text{(A18)}$$

$$\langle v_f^{*2}\rangle=v_f^2+(m/M^*)^2\langle v_{\text{c.m.}}^2\rangle. \quad \text{(A19)}$$

Since v_f and $v_{\text{c.m.}}$ are of the same order (see Appendix I), the correction terms above are very small. The averages of both v_f^* and v_f^{*2} differ by only about 0.01% from the initial values, before isotropic neutron emission.

Although neutron emission thus makes little change in the average fragment velocity, it does introduce a spread into the resulting fragment velocities. This may be evaluated, for emission of one neutron, from Eqs. (A18) and (A19):

$$\sigma^2(v_f^*)=\tfrac{1}{3}(m/M^*)^2\langle v_{\text{c.m.}}^2\rangle+\cdots. \quad \text{(A20)}$$

The variance of v_f^* may be rewritten as a relative variance in terms of energies, neglecting the difference between initial and final fragment masses:

$$(1/v_f^{*2})\sigma^2(v_f^*)\cong mA\bar{E}_{\text{c.m.}}/3M_HM_LE_K. \quad \text{(A21)}$$

[89] V. N. Nefedov, Zhur. Eksp. i Teoret. Fiz. **38**, 1657 (1960) [translation: Soviet Phys.—JETP **11**, 1195 (1960)].

[90] W. M. Gibson, T. D. Thomas, and G. L. Miller, Phys. Rev. Letters **7**, 65 (1961).

In this equation the symbols M_H, M_L, E_K, and A are the same as used in Appendix I, and, as before, the difference between mass and mass number M is neglected. The variance above is that produced by the emission of one neutron, and should be multiplied by ν_f to apply to the emission of ν_f neutrons by a fragment.

The mass resolution of a time-of-flight experiment is given by[6]

$$\sigma^2(M)=(M_HM_L/A)^2 \times[(1/v_H^2)\sigma^2(v_H)+(1/v_L^2)\sigma^2(v_L)], \quad \text{(A22)}$$

if the over-all experimental dispersions $\sigma^2(v_L)$ and $\sigma^2(v_H)$ are independent, and small. Thus the mass resolution due to neutron emission alone, without considering other sources of error, is given by

$$\sigma^2(M)\cong M_HM_Lm\bar{E}_{\text{c.m.}}\nu/3AE_K. \quad \text{(A23)}$$

This variance is nearly a constant for most fragment masses, since the total neutron emission $\nu(M_H)$ does not change greatly, and the variation of E_K is roughly the same as that of M_HM_L.

Results similar to Eq. (A23), though less general, have been derived both by Stein and Whetstone[7] and by Milton and Fraser.[9] The dispersion in mass for time-of-flight data given by Eq. (A23) is small, with $\sigma^2(M)$ amounting to 0.3 for $U^{235}+n$ and 0.6 for Cf^{252}, from neutron emission effects alone. Other sources of experimental dispersion, including timing accuracy and foil thickness, have comparable effects on the mass resolution in the best time-of-flight work. The effects of independent errors in measuring the two fragment velocities are easily calculated from Eq. (A22).

The mass resolutions used in correcting time-of-flight data in this paper were based mainly on these equations. The resulting figures were, except for Cf^{252}, $\sigma^2(M)=0.8$ for the Chalk River data[22] and 1.2 for the Los Alamos data,[21] corresponding to resolution functions of 2.1 and 2.6 mass units full width at half-maximum; for Cf^{252} a resolution correction of $\sigma^2(M)=1.4$ was used in both cases,[8,9] corresponding to 2.8 mass units full width at half-maximum. These resolution widths, although independently calculated, are essentially as estimated by the experimentalists.

B. Fragment Energy Data

Fission fragment masses determined by the ratios of final fragment energies are subject to much more inherent dispersion than the velocity measurements just discussed. This large mass dispersion is primarily due to the appreciable shift in fragment energy which is caused by neutron emission. From Eq. (A17), the change ΔE_M in fragment energy caused by the emission of one neutron is[1]

$$\Delta E_M=-E_f+(m/M^*)E_{\text{c.m.}}-2(E_fE_{\text{c.m.}})^{\frac{1}{2}}\cos\theta_{\text{c.m.}}. \quad \text{(A24)}$$

The assumptions of isotropic emission and no correlation between $E_{\text{c.m.}}$ and $\theta_{\text{c.m.}}$ give the average energy shift for a given mass, for one neutron emitted,

$$\langle\Delta E_M\rangle=-E_f+(m/M^*)\bar{E}_{\text{c.m.}}. \quad \text{(A25)}$$

If the fragment masses are determined in the usual manner by the equation

$$M_H/M_L=E_L/E_H, \quad \text{(A26)}$$

using the measured energies E_L^* and E_H^* instead of the initial fragment energies E_L and E_H, the average error in calculated heavy-fragment mass M_{HC} will thus amount to

$$M_{HC}-M_H\equiv\Delta M_H=-\Delta M_L \cong(M_L\nu_H-M_H\nu_L)/A, \quad \text{(A27)}$$

for any given fragment mass. This shift amounts on the average only to about -0.25 mass units, for M_H, but is by no means constant with mass. Because of the variation of $\nu_f(M)$ with fragment mass the apparent mass shift changes from $\Delta M_H\cong-1$ at low mass ratios to about $+1$ at high mass ratios. Thus the calculation of fragment mass by the ratio of energies has the effect of widening the apparent mass spectrum, due to the correlation of ν_f and M.

There is also a broadening in the apparent fragment mass even for a single initial mass, due both to varying directions and numbers of the emitted neutrons. This can be calculated to give the conditional variance

$$\sigma^2(M_{HC};M_H)=(4M_LM_Hm\bar{E}_{\text{c.m.}}\nu/3AE_K) +(M_Hm/A)^2\sigma^2(\nu_L;M_L) +(M_Lm/A)^2\sigma^2(\nu_H;M_H)+\cdots \quad \text{(A28)}$$

for any given mass ratio. However, this variance is essentially constant with mass, and may be accurately approximated by the average,

$$\langle\sigma^2(M_{HC};M_H)\rangle\cong(\bar{E}_{\text{c.m.}}\bar{\nu}/3\bar{E}_f)+\tfrac{1}{4}\sigma^2(\nu), \quad \text{(A29)}$$

in which the difference of the neutron mass m from 1.0 has been neglected, and other approximations have been made. The first term in Eq. (A28) is just four times larger than the corresponding variance of masses calculated from velocity ratios [Eq. (A23)]. As was pointed out in Sec. III–C, $\sigma^2(\nu_L;M_L)$ and $\sigma^2(\nu_H;M_H)$ have not been directly measured yet; the approximation $\frac{1}{4}\sigma^2(\nu)$ given in Eq. (A29) is based on the assumption of no conditional correlation of ν_L and ν_H (i.e., for a given mass ratio), and on negligible correlation of ν and M_H. The broadening given by Eq. (A28) or Eq. (A29) amounts to $\sigma^2\cong1.6$ for $U^{235}+n$, and to ~2.8 for Cf^{252}.

However, the major part of the over-all broadening of the apparent mass spectrum is due to the correlation of ν_f and M, as mentioned above. The over-all variance of M_{HC}, the heavy-fragment mass as calculated from final energies, may be shown to be

$$\sigma^2(M_{HC})=\sigma^2(M_H)\{1+[\bar{M}_H\langle d\nu_L/dM_L\rangle +\bar{M}_L\langle d\nu_H/dM_H\rangle-\bar{\nu}]/A\}^2+(\bar{E}_{\text{c.m.}}\bar{\nu}/3\bar{E}_f) +\tfrac{1}{4}\sigma^2(\nu)+\cdots. \quad \text{(A30)}$$

This does not include any ordinary sources of experimental error, but is due solely to neutron emission effects on the fragment energies.

These neutron effects lead to a fragment mass variance for either peak, for fission of $U^{235}+n$, of 36.2 ± 3, based on a true variance of 30.8 ± 2 and the various other numerical values[91] given in Tables I and II. In this case neutron emission widens the apparent mass distributions (if calculated from energy ratios) by $\sigma^2(M)=5.4\pm1.4$, almost an order of magnitude larger than for time-of-flight data. The calculated resultant variance of 36.2 ± 3 for $U^{235}+n$ may be compared with experimental figures of 37.5 ± 1 for the double-ion-chamber data of Apalin *et al.*[13] (after correcting for grouping of data[10]), and 33.9 ± 1 for the semi-conductor counter data of Gibson, Thomas, and Miller.[90,92]

For Cf^{252} fission, neutron effects on fragment energy data should widen the resulting mass data by $\sigma^2(M)=10.8\pm4$, using the values[91] in Tables I and II. This would increase the mass variance from 47.6 ± 4 to 58.4 ± 6.

Because of these large effects of neutron emission, mass distributions determined from fragment energy ratios are not very reliable if uncorrected. Correction depends on knowledge of $\nu_f(M)$, which does not yet exist for many fissioning nuclides. However, where energy-ratio data and another type of mass data (either on final masses, or velocity measurements on initial masses) are both accurately known for the same nuclide, it should be possible to obtain some information on $\langle d\nu_L/dM_L\rangle$ and $\langle d\nu_H/dM_H\rangle$ from the differences in the two types of data. As an example of this method, the energy-ratio data of Gibson *et al.*[90,92] on $U^{235}+n$, and the time-of-flight data of Fraser and Milton,[22] and of Stein,[21] yield the average value, $\frac{1}{2}\langle d\nu_L/dM_L\rangle+\frac{1}{2}\langle d\nu_H/dM_H\rangle=0.03\pm0.04$. This does not yet have enough accuracy to be interesting. However, better data might give more detail, particularly if *cumulative* mass distributions from energy-ratios are used, with the apparent mass shift given by Eq. (A27).

For fine details of mass distributions, however, it is obvious that velocity measurements are inherently better. The shifts of apparent mass occurring in energy data can create apparent peaks of mass yield where none exist, or can eliminate true peaks in mass yield. These effects have been verified numerically by applying the effects of mass shift and dispersion to time-of-flight mass data so as to obtain the corresponding mass data from energy ratios. It is found that any correspondence between the original fine structure of mass yield and that given by energy ratios is largely coincidental.

[91] The numerical values used for $\langle d\nu_L/dM_L\rangle$ and $\langle d\nu_H/dM_H\rangle$ are the "indirect" values given first in Table I, calculated from mass yields.

[92] T. D. Thomas (private communication).